Journal of South American Earth Sciences 28 (2009) 239–262

Contents lists available at ScienceDirect

Journal of South American Earth Sciences

journal homepage: www.elsevier.com/locate/jsames

Provenance of the late Proterozoic to early Cambrian metaclastic sediments of the Sierra de San Luis (Eastern Sierras Pampeanas) and Cordillera Oriental, Argentina

Malte Drobe [a,*], Mónica G. López de Luchi [b,1], André Steenken [c,2], Robert Frei [d,3], Rudolf Naumann [e,4], Siegfried Siegesmund [a], Klaus Wemmer [a]

[a] Geoscience Centre of the Georg-August-Universität, Goldschmidtstr. 3, 37077 Göttingen, Germany
[b] Instituto de Geocronología y Geología Isotópica, INGEIS, Pabellón INGEIS, Ciudad Universitaria, C1428EHA, Buenos Aires, Argentina
[c] Institut für Geographie und Geologie, Universität Greifswald, Friedrich-Ludwig-Jahn-Str. 17A, 17487 Greifswald, Germany
[d] Institute of Geography and Geology, University of Copenhagen, Nordic Center for Earth Evolution (NordCEE), Øster Voldgade 10, 1350 Copenhagen K, Denmark
[e] GFZ Potsdam, Telegraphenberg 327 B, 14473 Potsdam, Germany

ARTICLE INFO

Article history:
Received 15 December 2008
Accepted 1 June 2009

Keywords:
Provenance
Tectonic setting
Eastern Sierras Pampeanas
Puncoviscana Formation
Gondwana margin

ABSTRACT

Provenance studies have been performed utilising major and trace elements, Nd systematics, whole rock Pb–Pb isotopes and zircon U/Pb SHRIMP data on metasedimentary rocks of the Sierra de San Luis (Nogolí Metamorphic Complex, Pringles Metamorphic Complex, Conlara Metamorphic Complex and San Luis Formation) and the Puncoviscana Formation of the Cordillera Oriental. The goal was the characterisation of the different domains in the study area and to give insights to the location of the source rocks. An active continental margin setting with typical composition of the upper continental crust is depicted for all the complexes using major and trace elements. The Pringles Metamorphic Complex shows indications for crustal recycling, pointing to a bimodal provenance. Major volcanic input has to be rejected due to Th/Sc, Y/Ni and Cr/V ratios for all units. The $\varepsilon Nd_{(540\ Ma)}$ data is lower for the San Luis Formation and higher for the Conlara Metamorphic Complex, as compared to the other units, in which a good consistency is given. This is similar to the T_{DM} ages, where the metapsammitic samples of the San Luis Formation are slightly older. The spread of data is largest for the Pringles Metamorphic Complex, again implying two different sources. The whole rock $^{207}Pb/^{206}Pb$ isotopic data lies in between the South American and African sources, excluding Laurentian provenances. The whole rock Pb–Pb data is almost indistinguishable in the different investigated domains. Only the PMC shows slightly elevated $^{208}Pb/^{204}Pb$ values. Possible source rocks for the different domains could be the Quebrada Choja in the Central Arequipa–Antofalla domain, the Southern domain of the Arequipa–Antofalla basement, the Brazilian shield or southern Africa. Zircon SHRIMP data point to a connection between the Puncoviscana Formation and the Conlara Metamorphic Complex. Two maxima around 600 Ma and around 1000 Ma have been determined. The Nogolí Metamorphic Complex and the Pringles Metamorphic Complex show one peak of detrital zircons around 550 Ma, and only a few grains are older than 700 Ma. The detrital zircon ages for the San Luis Formation show age ranges between 590 and 550 Ma. A common basin can be assumed for the Conlara Metamorphic Complex and the Puncoviscana Formation, but the available data support different sources for the rest of the Complexes of the Sierra de San Luis. These share the diminished importance or the lack of the Grenvillian detrital peak, a common feature for the late Cambrian–early Ordovician basins of the Eastern Sierras Pampeanas, in contrast to the Sierras de Córdoba, the PVF and the Conlara Metamorphic Complex.

1. Introduction

The geodynamic evolution of the southwestern margin of Gondwana, based on the geochemical and isotopic provenance studies of the (meta-) sediments, has been the focus of investigation for the last 10 years in the Eastern Sierras Pampeanas and the Cordillera Oriental (Sims et al., 1998; Rapela et al., 1998, 2007; López de Luchi et al., 1999, 2003; Bock et al., 2000; Brogioni, 2001; Aceñolaza et al., 2002; Cerredo and López de Luchi, 2002;

* Corresponding author. Fax: +49 551 39 9700.
E-mail addresses: mdrobe@gwdg.de (M. Drobe), deluchi@ingeis.uba.ar (M.G. López de Luchi), asteenken@gmail.com (A. Steenken), robertf@geol.ku.dk (R. Frei), rudolf@gfz-potsdam.de (R. Naumann), ssieges@gwdg.de (S. Siegesmund), kwemmer@gwdg.de (K. Wemmer).
[1] Fax: +54 11 4783 3024.
[2] Fax: +49 3834 86 4572.
[3] Fax: +45 35 32 24 40.
[4] Fax: +49 331 288 1474.

0895-9811/$ - see front matter © 2009 Elsevier Ltd. All rights reserved.
doi:10.1016/j.jsames.2009.06.005

Thomas et al., 2002; Thomas and Astini, 2003; Finney et al., 2003; Schwartz and Gromet, 2004; Steenken et al., 2004, 2006; Zimmermann, 2005; Escayola et al., 2007; Adams et al., 2008). Several scenarios like passive or active margin settings as well as autochthony or allochthoneity were suggested for the Neoproterozoic to early Palaeozoic evolution of the metaclastic units of the Eastern Sierras Pampeanas and the Cordillera Oriental, two of the main morphotectonic units along the southwestern margin of Gondwana in Argentina (e.g. Ramos, 1988; Bahlburg, 1990; Astini et al., 1995; Pankhurst and Rapela, 1998; Rapela et al.,1998, 2007; Bock et al., 2000; Lucassen et al., 2000; Zimmermann and Bahlburg, 2003; López de Luchi et al., 2003; Schwartz and Gromet, 2004; Steenken et al., 2004, 2006; Prozzi and Zimmermann, 2005; Zimmermann, 2005; Schwartz et al., 2008; Adams et al., 2008; Casquet et al., 2008).

Geochemical and isotope studies (e.g. Schwartz and Gromet, 2004; Steenken et al., 2004; Zimmermann, 2005) support the hypothesis that large parts of the low to high-grade metaclastic successions of the Eastern Sierras Pampeanas (Fig. 1) constitute an extension of the Puncoviscana Formation, the very low to low-grade metaclastics of northwestern Argentina and southernmost Bolivia. Metamorphism, deformation and magmatism affecting these metaclastic units result from the early Palaeozoic Pampean orogenic cycle (Toselli and Aceñolaza, 1978; Aceñolaza and Toselli, 1981; Omarini, 1983; Aceñolaza et al., 1988, 1990; Rapela et al., 1998, 2007; Bock et al., 2000; Steenken et al., 2004, 2006, 2007; Zimmermann, 2005).

The investigation of the geochemical characteristics of (meta-) clastic deposits is suitable to constrain not only the tectonic setting, but also the geological provinces from which the clastic material was eroded. Studies to solve provenance related problems of (meta-) clastic sediments can be carried out in different ways: (i) lithoclasts may be analysed statistically in thin sections (Dickinson and Suczek, 1979; Zimmermann, 1999; von Eynatten et al., 2003), (ii) the major and trace element composition of the whole rock and mineral samples may be considered (e.g. Floyd and Leveridge, 1987; McLennan et al., 1990, 1993; Zimmermann, 1999), and (iii) isotopic whole rock systems like Pb–Pb or Sm–Nd and single grain studies such as U–Pb dating of zircons can also be applied.

The advantage of trace elements in contrast to major elements is the coherent behaviour of specific element groups, like the HFSE (including the REE) during weathering, diagenesis and metamorphism. The fact that those elements are insoluble at surface conditions as well as during metamorphic processes makes them far more reliable in ascertaining the provenance of the clastic material and the different tectonic settings where they are deposited (e.g. Bhatia, 1983; Taylor and McLennan, 1985; McLennan et al., 1993; Roser et al., 1996). REE, Ni, Y, Sc, Cr, Th, V, Ti, Hf and Zr are most commonly used in the discrimination between different tectonic settings and/or sources. Contributions of acidic or basic material to the sediments, as well as the degree of recycling may be identified by specific elements. Ratios between certain trace elements will reflect the different contributions to the clastic material characterising the geotectonic setting from where they were derived or

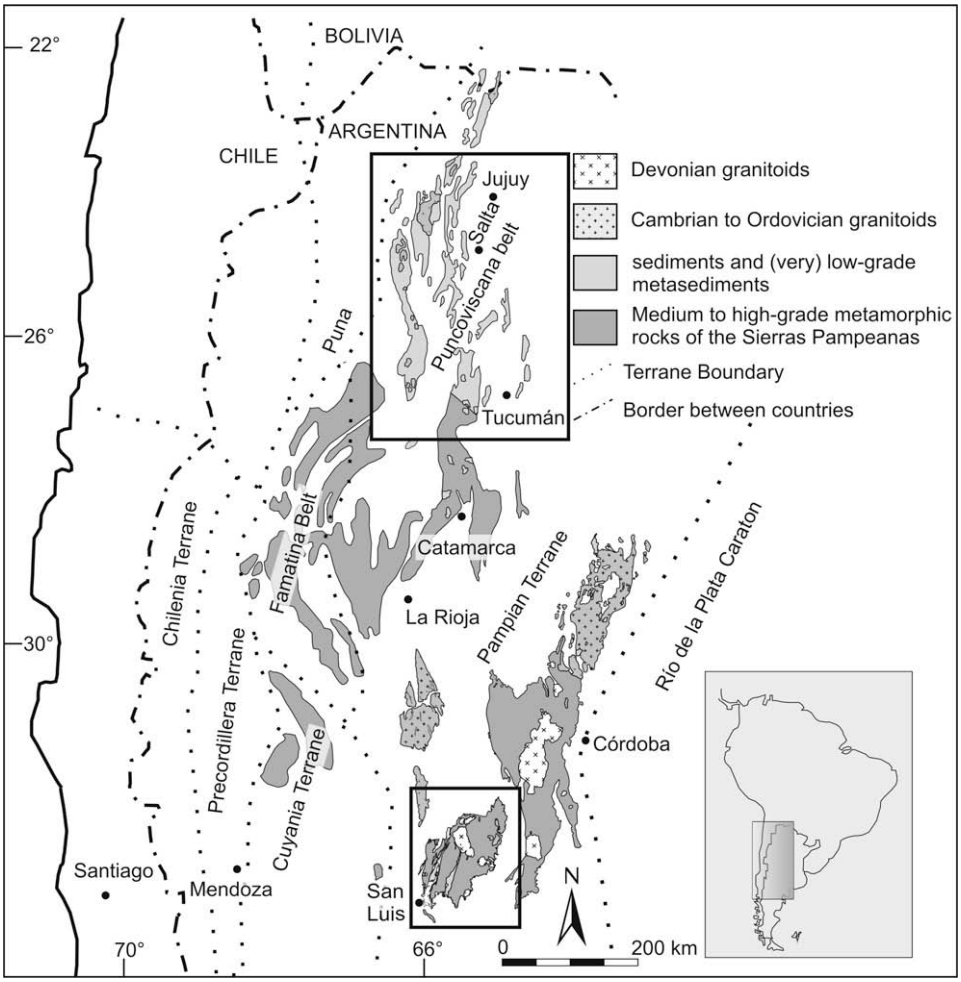

Fig. 1. Geological sketch of the Eastern Sierras Pampeanas and the Puncoviscana belt and the main terranes west of the Río de la Plata Craton (modified after Lucassen et al., 2000; Rapela et al., 2007; Ramos, 2008). Boxes mark the study areas.

in which they were deposited. However, discrimination between source rock characteristics and the plate tectonic setting is not that easy to establish. The combination of Nd and Pb isotopes with major and trace elements provides the possibility for examining the geological setting of the provenance area and to determine the different terranes, their boundaries and origins. SHRIMP dating of zircon yields characteristic inheritance patterns reflecting the detritus of different orogenic events in the provenance area of the sediments. Therefore, the SHRIMP data provide an additional constraint to discriminate between different tectonic provinces that might show similar whole rock Nd and Pb isotope ratios.

The aim of this study is to provide new insights on the Ediacaran/early Palaeozoic geodynamic evolution along a part of the southwestern margin of Gondwana. Major and trace elements, Nd and Pb isotope systematics as well as SHRIMP U/Pb zircon data are used to both characterise and to show differences and/or similarities in the provenance and the tectonic setting of the Puncoviscana Formation (Cordillera Oriental) and higher-grade metaclastic sediments from the Sierra de San Luis [southern tip of the Eastern Sierras Pampeanas (Fig. 1)]. Previously suggested tectonic models for the early Palaeozoic evolution of the Pacific margin of Gondwana will be discussed by the combination of data presented here and results already published (e.g. Rapela et al., 1998; Sims et al., 1998; López de Luchi et al., 1999, 2003; Bock et al., 2000; Brogioni, 2001; Steenken et al., 2004, 2006; Prozzi and Zimmermann, 2005; Zimmermann, 2005; Rapela et al., 2007; Adams et al., 2008).

2. Geological setting

The Eastern Sierras Pampeanas (Fig. 1) consist of uplifted basement blocks, produced by Miocene to recent flat-slab subduction in the 27–33°30′S Andean segment (Ramos et al., 2002). The eastern belt of this morphostructural unit is known as the Pampean orogen, which is characterised by late Neoproterozoic sedimentation and Cambrian deformation, magmatism and metamorphism. The western sector, the Famatinian orogen, is characterised by Upper Cambrian to Middle Ordovician marine sedimentation and conspicuous Early Ordovician magmatism (Rapela, 2000). From 22°S to 27°S the Pampean belt at the Cordillera Oriental (Fig. 2) is dominated by the Puncoviscana Formation. Possible higher-grade metamorphic equivalents are exposed between 27° and 33°S, up to the southern extremes of the Eastern Sierras Pampeanas in the provinces of Córdoba and San Luis (Rapela et al., 1998, 2007; Schwartz and Gromet, 2004; Steenken et al., 2004; Zimmermann, 2005).

The Puncoviscana Formation (PVF), a belt of very low to low-grade metasediments, grading from slates to schists, is exposed along 800 km in northwestern Argentina (Fig. 2) from the Bolivian border north of 22°S up to the city of Tucumán at 27°S. This several 1000-m thick metasedimentary sequence is recorded in the Puna and adjacent Cordillera Oriental, and is mainly composed of siliciclastic flysch-like turbidites and pelagic clays. An Ediacaran/early Cambrian age has been inferred from *Oldhamia* ichnofossils and other traces (Aceñolaza and Durand, 1986; Durand, 1996; Aceñolaza and Tortello, 2003). The minimum sedimentation age of the PVF is given by the intruding 536 ± 7 Ma and 534 ± 9 Ma (U/Pb zircons) syn- to post-orogenic calc-alkaline granites (Bachmann et al., 1987). Lork et al. (1990) obtained ages from lower intercepts of detrital zircons at 560–530 Ma, placing a maximum age for the deposition of the PVF. The upper intercept from these zircon analyses denotes a late Palaeoproterozoic inheritance. The LA ICP-MS U/Pb zircon dating revealed population maxima at

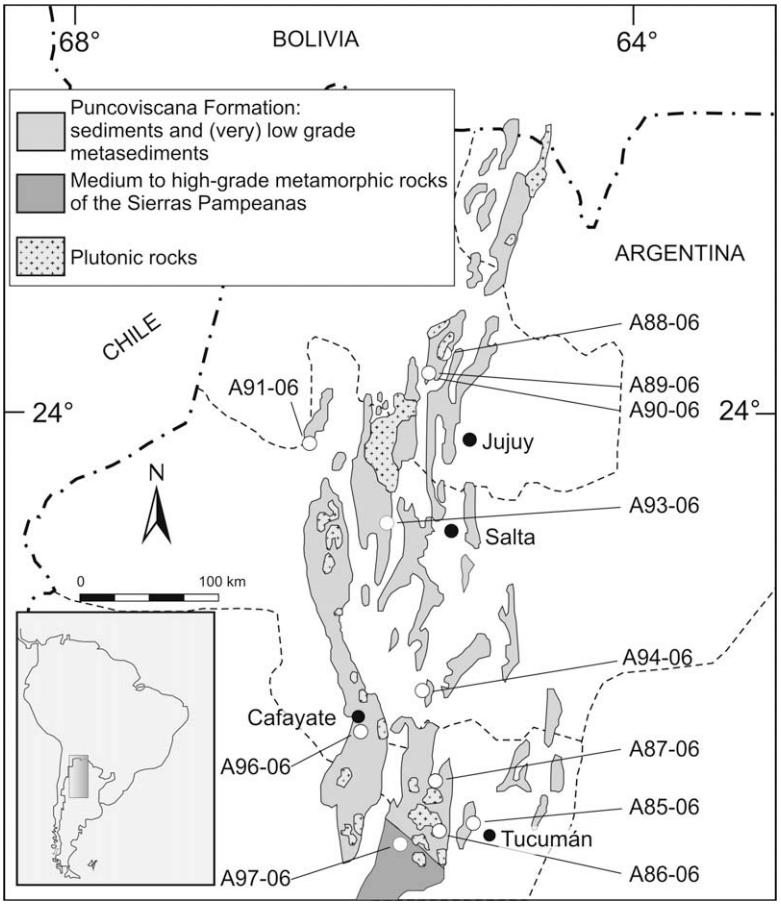

Fig. 2. Distribution of the Puncoviscana Formation (modified after Aceñolaza and Aceñolaza, 2005) and the location of the collected samples (white circles).

1100–1000 Ma, 650–600 and at 550–500 Ma, with minor populations throughout the Meso- and Palaeoproterozoic (Adams et al., 2006, 2008).

The Sierra de San Luis consists of three principal NNE trending metamorphic complexes (Fig. 3): the Nogolí (NMC), Pringles (PMC), and Conlara (CMC) Metamorphic Complexes. These units are separated by two narrow low-grade belts of the San Luis Formation (SLF) which is described by Prozzi and Ramos (1988). The complexes are mainly built up by greenschist to granulite facies metaclastic rocks. Only the NMC is dominated by orthogneisses. The metamorphic units are invaded by Ordovician and Devonian intrusives. The opening of Carboniferous continental basins defined the end for the ductile deformation and the compressive tectonic movements. Ordovician (Famatinian) back-arc mafic (noritic gabbros) to (ultra) mafic rocks (dunites, pyroxenites, hornblendites) and island-arc amphibolites are located in the PMC associated with granulite facies metaclastic rocks (Sims et al., 1997; Hauzenberger et al., 2001). During the last three decades a large number of studies have focused on the structural evolution, metamorphism and magmatism of the basement complexes in the Sierra de San Luis (Kilmurray and Dalla Salda, 1977; López de Luchi, 1987, 1996; Ortiz Suárez et al., 1992; Llambías et al., 1998; Sims et al., 1998; von Gosen and Prozzi, 1998; Delpino et al., 2001, 2007; López de Luchi et al., 2003, 2004, 2007; González et al., 2002; Steenken et al., 2004, 2006, 2008).

The geodynamic evolution and temporal relationship of the CMC and SLF with the more western PMC and NMC are still unsolved problems. The minimum age for the deposition of the CMC is provided by a $^{238}U/^{206}Pb$ SHRIMP detrital zircon age of 587 ± 7 Ma (Steenken et al., 2006). U/Pb zircon data for the PMC points to a maximum deposition age at ~530 Ma (Sims et al., 1998; Steenken et al., 2006), similar to the conventional zircon age of 529 ± 12 Ma for strata bound layers of metavolcanites in the SLF (Söllner et al., 2000). Mesoproterozoic or even older ages for the deposition of the NMC was assigned on the basis of the presence of banded iron formations and olivine spinifex-structures

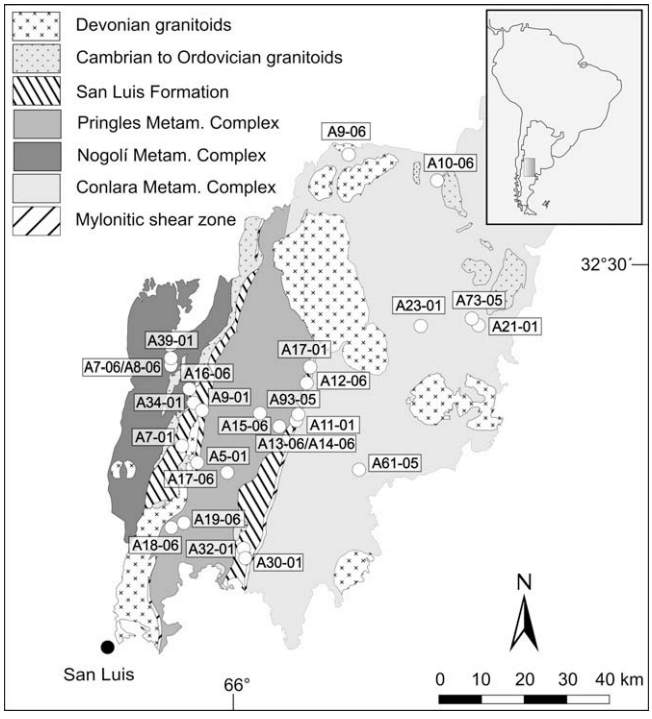

Fig. 3. Geological sketch of the Sierra de San Luis Palaeozoic units (modified after Steenken et al., 2006) with the different basement domains and intrusions. Sample location points are shown (white circles).

in komatiites (Sato et al., 2001; González et al., 2002). Recent SHRIMP zircon data on the crystallisation of the komatiite shed doubt on this old crystallisation age (Sato et al., 2006). Mesoproterozoic ages could not be determined by Steenken et al. (2006), who reported a concordant Pampean peak for detrital zircons in the PMC (545 Ma) and also a Famatinian overprint (498 Ma) in zircons. This is similar to the NMC, where Steenken et al. (2006) reported concordant monazite ages of 484 Ma and 473 Ma. No pre-Pampean metamorphic ages were found.

Geochronological constraints suggest that peak metamorphic conditions for the CMC were obtained during the Pampean orogeny (Steenken et al., 2005, 2006, 2007). Folded xenoliths of the D2 banded schists are observed in pervasively solid-state deformed granitoids like the Early Ordovician (497 ± 8 Ma) El Peñón batholith (Steenken et al., 2006). On the other hand, granulite facies metamorphism of the PMC that is associated with a near isobaric P–T path was dated as late Cambrian–early Ordovician (Steenken et al., 2007) based on a concordant U/Pb age of 498 ± 10 Ma.

Toselli (1990), Willner (1990), Rapela et al. (1998) and Söllner et al. (2000) argued for the SLF as an equivalent for the PVF, whereas Steenken et al. (2004, 2006) and Prozzi and Zimmermann (2005) demonstrated isotopic and geochemical similarities between the CMC and the PVF. Schwartz and Gromet (2004) proposed a comparable isotopic signature for the PVF and the metasedimentary rocks from northern and northwestern parts of the Sierras de Córdoba.

The early Palaeozoic accretional history along the proto-Andean margin of Gondwana is interpreted as a protraction of the Pan-African–Brasiliano orogeny (Leite et al., 2000; Janasi et al., 2001). The Pampean orogenic cycle between 535 and 510 Ma (Ramos, 1988; Rapela et al., 1998) was triggered by the tectonic emplacement of the Pampean terrane along the southwestern margin of the Río de La Plata craton. The Pampean orogen in the Eastern Sierras Pampeanas contains two belts, an eastern calc-alkaline magmatic belt and a western peraluminous granite/high-grade metasedimentary belt. The resumption of subduction along the western margin of the Pampean terrane in the late Cambrian and the subsequent Middle Ordovician amalgamation of the Cuyania and/or Precordillera Terrane constitutes the Famatinian orogenic cycle (Ramos et al., 1986; Sims et al., 1998). This cycle was locally associated with late Cambrian sedimentation (Steenken et al., 2006).

Collisional and non-collisional models were proposed for the Pampean orogen and consequently different tectonic settings and provenances were assigned to the Ediacaran–early Cambrian metaclastic units preceding the development of the Pampean orogen. Discontinuous strings of mafic to ultra-mafic bodies with a MORB-type geochemical signature in association with a metasedimentary sequence of pelitic migmatites and amphibolites were interpreted as a disrupted ophiolitic sequence (Escayola et al., 1996, 2007; Ramos et al., 2000), supporting the existence of a Neoproterozoic oceanic lithosphere along the southwestern margin of Gondwana. Collisional models considered that the metaclastic units i.e. the PVF were deposited along a passive margin that later turned into an active margin. Rapela et al. (1990) proposed that the PVF developed along the passive margin of the Rio de la Plata craton. The distribution of different sedimentary facies led to the proposition of an aulacogenic origin of the sediments with a possible triple junction amid the Arequipa–Antofalla, Amazonian and Río Apas cratons (Rapela et al., 1998; Ramos, 2008). Rapela et al. (1998) advocate subduction and the accretion of the Pampean terrane, an allochthonous or para-autochthonous (originally rift-related) Mesoproterozoic to Neoproterozoic continental fragment, to the western margin of Gondwana. In this model, calc-alkaline magmatism of the Sierra Norte de Córdoba was associated with east-dipping subduction and ended with the collision of the Pampean terrane. Sims et al. (1998) and Stuart-Smith et al.

(1999) suggested that the Pampean orogenic cycle involved overthrusting of a passive marginal basin eastwards over the Río de la Plata craton. However, the prolonged igneous activity with dominant felsic calc-alkaline granitoids of the Sierra Norte de Córdoba resulted from a post-collisional extension and melting of older I-type source rocks. Ramos (2008 and references therein) considered that the Puncoviscana trough was a peripheral foreland basin related to the collision along the Eastern Sierras Pampeanas of the Pampia block with the Río de La Plata craton. A non-collisional hypothesis were summarised by Schwartz et al. (2008) who proposed a 555–525 Ma east-dipping subduction and arc activity that ended with a ridge-trench collision, beginning at 525 Ma. This process initiated a short-lived magmatic/metamorphic event in the accretionary prism, i.e. in the Pampean orogen. Rapela et al. (2007) and Casquet et al. (2008) recently suggested that the PVF was probably a fore-arc sedimentary sequence that had developed on the southern and western margins of the Kalahari craton. It was moved to its present position by the collision of the Western Sierras Pampeanas Terrane, a part of the Amazonas and Arequipa cratons.

Attempts to constrain the provenance of the PVF based on major and trace elements and sedimentological studies (Aceñolaza et al., 1983; Willner et al., 1985; Ježek and Miller, 1986; Rossi de Toselli et al., 1997; Do Campo and Ribeiro Guevara, 2002) infer a passive continental margin of the Río de la Plata craton with turbidity currents, which were fed from the east for the deposition of the PVF. Geochemical data from volcanic rocks from different levels of the PVF point to a change from a rift environment to a back-arc setting (Omarini et al., 1999). Kraemer et al. (1995) and Keppie and Bahlburg (1999) argued for a foreland basin infill that was corroborated by a large collection of REE, major and trace element data (Zimmermann, 2005). Based on Nd and Pb isotope systematics, a major contribution of mantle-derived volcanic rocks was excluded (Bock et al., 2000).

Contrasting zircon inheritance patterns and Nd model ages between 1.8 and 1.6 Ga for the PVF and the metaclastic units of the Eastern Sierras Pampeanas (Bock et al., 2000; Schwartz and Gromet, 2004; Steenken et al., 2004, 2006, 2008; Adams et al., 2006, 2008; Escayola et al., 2007; Rapela et al., 2007) argue against the Río de La Plata craton being a source for the metasediments of the PVF as it was previously suggested by Rapela et al. (1998). T_{DM} ages from the Río de la Plata craton are between 2.8 and 2.3 Ga (Hartmann et al., 2002; Pankhurst et al., 2003; Rapela et al., 2007). Brito Neves et al. (1999), and Schwartz and Gromet (2004) proposed an origin of the Puncoviscana sediments in the vicinity of the Amazonia craton. Escayola et al. (2007) argued for an intra-oceanic island-arc between the Río de La Plata craton and the Pampean terrane, inhibiting the supply of Palaeoproterozoic material from the craton to the metasedimentary units of the Sierras Pampeanas. Based on geochemical information, Zimmermann (2005) proposed an active continental margin for the PVF with west directed sedimentation by deposition into a foreland basin with the magmatic arc in the east, on the margin of the Río de la Plata craton. This palaeogeographic configuration would block or at least restrict sediment supply from further east, leading to sediments of active margins and diminish the amount of passive margin sediments. The models of Rapela et al. (2007) and Casquet et al. (2008) suggest that the PVF was probably a fore-arc sedimentary sequence that had developed on the southern and western margins of the Kalahari craton. Consequently, sources from the Kalahari craton should be examined in detail, to clearly check its comparability to the Eastern Sierras Pampeanas.

3. Sample material

A total of 36 samples of metasedimentary rocks from the PVF and the metamorphic units of the Sierra de San Luis were analysed for major and trace elements with ICP-MS and XRF (Table 1). Sm–Nd model ages were calculated for 22 of these samples. The Pb isotopic composition was calculated for 23 whole rock samples. The SHRIMP technique was applied on four samples (A73-05, A93-05, A7-06 and A8-06). The locations are indicated in Figs. 2 and 3.

3.1. Nogolí Metamorphic Complex

The NMC is built up mainly by felsic orthogneisses. Mafic gneisses are subordinate. Only few paragneisses could be observed. At the outcrop scale D_2 tight folding around steeply inclined axes could be observed. von Gosen and Prozzi (1998) described this deformation event as previous to the Famatinian orogenic cycle. Three metapsammitic samples (A7-06, A8-06 and A16-06) and one metapelitic (A39-01) sample of non migmatitic rocks were collected in the northeastern of the NMC. The main mineral assemblage is quartz, plagioclase, biotite and muscovite with accessory minerals like zircon, apatite, ±clinozoisite and ±sillimanite. Two foliations are visible in thin sections, both defined by biotite. Locally, consumption of mica due to sillimanite growth indicates the peak metamorphic conditions. Randomly oriented muscovite flakes are recognised (von Gosen and Prozzi, 1998).

3.2. Pringles Metamorphic Complex

The PMC mostly consists of para-, orthogneisses and mica-schists with less abundant amphibolites (Ultra) mafic complexes are located along a belt in the western sector of the complex and exhibit a spatial and temporal connection with the granulite facies rocks (Hauzenberger et al., 2001; Steenken et al., 2007).

Six samples were obtained. Three of them are metapsammitic rocks (A13-06, A14-06 and A19-06), one is a metapelite (A15-06)

Table 1
Average major element and trace-element ratios for the different domains of the Sierra de San Luis and the Puncoviscana Formation of the Cordillera Oriental.

	NMC		PMC		CMC	SLF		PVF	
	Metapsammite (n = 3)	Metapelite (n = l)	Metapsammite (n = 5)	Metapelite (n = l)	Metapsammite (n = 6)	Metapsammite (n = 2)	Metapelite (n = 6)	Metapsammite (n = 9)	Metapelite (n = 2)
SiO_2	76.7	54.9	78.8	59.4	70.6	79.1	60.7	70.8	61.1
$A1_2O_3$	11.0	20.2	10.2	18.5	12.6	10.5	18.5	13.0	17.4
Th/Sc	1.5	1.1	3.3	1.1	1.1	1.9	1.2	1.2	0.7
La/Th	2.6	2.4	2.0	2.5	2.8	2.1	2.4	2.7	2.3
Ti/Zr	28.1	49.1	22.8	48.6	30.0	26.3	53.9	31.3	55.6
La/Sc	3.9	2.5	5.3	2.8	3.2	3.8	2.9	3.3	1.7
Cr/Ni	2.6	2.6	4.0	2.0	2.6	1.2	2.3	2.6	2.4
Y/Ni	1.6	0.8	2.9	0.6	1.2	2.4	0.5	1.4	0.7
Zr/Sc	23.0	13.8	67.8	10.6	23.1	23.4	18.7	20.5	9.0
Eu/Eu^*	0.54	0.61	0.49	0.55	0.60	0.54	0.61	0.56	0.60

and two are metapsammopelites (A5-01 and A18-06). The metapsammitic samples A13-06 and A14-06 were taken in the eastern area, whereas A19-06 was taken in the southwest of the PMC. In some cases coarser and finer grained layers are observable. These are biotite–muscovite gneisses consisting of quartz, biotite, muscovite and plagioclase. The accessory minerals are zircon, apatite, ±garnet, ±tourmaline and ±titanite. The metapsammopelitic samples were taken in the southwest (A18-06) and in the central area (A5-01). Interlayering of psammitic and pelitic layers is characteristic for these rocks. These sheets are sheared and occur as lenses or disrupted layers. The psammitic parts are highly enriched in quartz with minor plagioclase. In these layers elongated biotite and muscovite grains are unevenly distributed. The pelitic layers consist of strongly bent muscovite and biotite, which show an s-c fabric. The metapelitic sample A15-06 is a greyish rock composed of biotite, quartz, K-feldspar, plagioclase and sillimanite. Accessory minerals are zircon, apatite and a relatively high amount of opaque minerals. Biotite and sillimanite define layers that are often sheared and rotated, alternating with quartz rich bands. Biotite reaction to fibrolite is recognised in the thin section.

3.3. Conlara Metamorphic Complex

The metamorphic series of the CMC comprises both metasedimentary and metaigneous rocks. The former are dominated by metagreywackes and scarce metapelites with lesser amounts of tourmaline schists and turmalinites. Samples from this complex are metapsammitic rocks, which are characterised by medium-grained layers of quartz and plagioclase and fine-grained layers, dominated by biotite (A21-01, A23-01, A61-05 and A10-06). A9-06 is a fine-grained, low-grade metapsammite. The banded schists (A21-01, A23-01 and A10-06) are characterised by a metamorphic layering defined by alternating mica and quartz domains.

The mica domains consist of green biotite, plagioclase, scarce quartz plus opaque minerals, apatite and zircon. Muscovite blasts occur as large flakes.

The quartz domains are made up of plagioclase, quartz and some biotite. Relic garnet is locally found in these domains.

3.4. San Luis Formation

The SLF comprises metapsammites and phyllites (Prozzi and Ramos, 1988). Black shales only occur subordinately and conglomerates are scarce. The sample material from this unit is either a metapsammitic (A9-01 and A12-06) or metapelitic (A7-01, A11-01, A17-01, A30-01, A32-01 and A34-01). Sample A17-06 is a volcanic rock of intermediate composition. The fine-grained metapsammitic samples consist of quartz, plagioclase, muscovite and biotite. The micas define the foliation. Quartz and plagioclase do not seem to be strongly affected by dynamic recrystallisation. A lot of quartz grains show static recrystallisation resulting in triple junctions. The phyllitic samples are characterised by thin layers of mica and more coarse-grained quartz layers that are interspersed with a fine-grained matrix. Furthermore, medium-grained, unevenly distributed quartz clasts are typical for these rocks. These clasts are all dynamically recrystallised parallel to the foliation.

3.5. Puncoviscana Formation

The PVF consists of very low to low-grade metasedimentary rocks in the northern area, while the southern area is built up by medium to high-grade metasedimentary rocks (Aceñolaza et al., 2000). The analysed samples vary from metapelitic (A85-06 and A86-06) to low-grade metapsammitic (A87-06, A88-06, A89-06 A90-06, A91-06, A93-06 and A94-06) and medium-grade metapsammitic rocks (A96-06 and A97-06).

The metapelitic rocks are greenish to greyish in colour. Both have a very high content of sericite, white mica and chlorite. In this matrix a varying degree of moderately rounded quartz and a few plagioclase and muscovite grains occur. Some samples only have a very few of these detrital clasts, others show silty layers that are dominated by these grains. In sample A85-06 some small microcracks affect the surrounding material as evidenced by the presence of brownish oxides. The metapsammites contain quartz, plagioclase and muscovite. These grains are surrounded by white mica and chlorite. Less abundant is calcite that occurs as grains in the normal sample material, but also as the main mineral assemblage in small joints. These were removed and not used for the analyses. The two medium-grade metapsammitic samples (A96-06 and A97-06) are banded schists, similar to those of the CMC (López de Luchi, 1986). The banding is made up of an interlayering of quartz and mica domains, similar to the CMC. In sample A97-06 two different types of biotite can be observed. One is brownish and platy, the other is greenish and fibrous. In this sample garnet could be observed in the coarse-grained layers.

4. Analytical results

4.1. Chemical index of alteration

Major elements are useful in provenance analyses if the rocks were not strongly affected by metamorphism, diagenesis or weathering (McLennan et al., 1993). Major elements may provide some indication of the sources for the clastic erosion material (e.g. Boles and Franks, 1979; Nesbit et al., 1996; Zimmermann and Bahlburg, 2003). The deviation from the original composition of the source material by alteration processes can be inferred from the chemical index of alteration (CIA) that is calculated with mol% as: $Al_2O_3/(Al_2O_3 + CaO^* + Na_2O + K_2O) \times 100$ (Nesbit and Young, 1982). The CaO^* indicates that only calcium from silicate minerals is considered. The CaO content from apatite and carbonate has to be subtracted. This is done by using the molar proportion of CO_2 and 10/3 of the molar proportion of P_2O_5. The CIA varies in the different rock types. Fresh granitic rocks e.g. show values between 45 and 55, whereas shales exhibit average values between 70 and 75 and pure chlorites go up to 100. The CIA displays the degree of feldspar weathering. The sample collection shows CIA values of 53–85, with an average for the metapsammitic rocks of 59 ($n = 25$), indicating moderate feldspar alteration and a mean for the metapelitic rocks of 71 ($n = 10$), indicating a high amount of clay minerals.

In a ternary plot of Al_2O_3, $CaO^* + Na_2O$ and K_2O, a trend parallel to the CN-A axis should be visible (Fig. 4) if no modification of the $CaO^* + Na_2O$ and K_2O ratio from a homogenous source took place. When looking at the main trend disregarding the single units, a deviation from the ideal weathering trend that runs parallel to the CN-A axis is visible. Different source rocks start their weathering trend at different positions in the ternary diagram. Assuming that the source for some rocks has a granitic composition, these rocks have to be on the right-hand side and samples with a tonalitic source will plot on the left-hand side (Fig. 4). The metapsammitic samples from López de Luchi et al. (2003) for the CMC or the ones for the PVF, for example, show a trend sub-parallel to the ideal weathering trend. According to the position in the CIA diagram, the source rocks from this collection define a trend, starting from granitic to granodioritic composition. A general change of the ratios from $CaO^* + Na_2O$ and K_2O is not visible.

4.2. Whole rock geochemistry

The metasedimentary rocks display a wide range (Table 1) of SiO_2 (55–88%) and Al_2O_3 (6–21%). Average major element

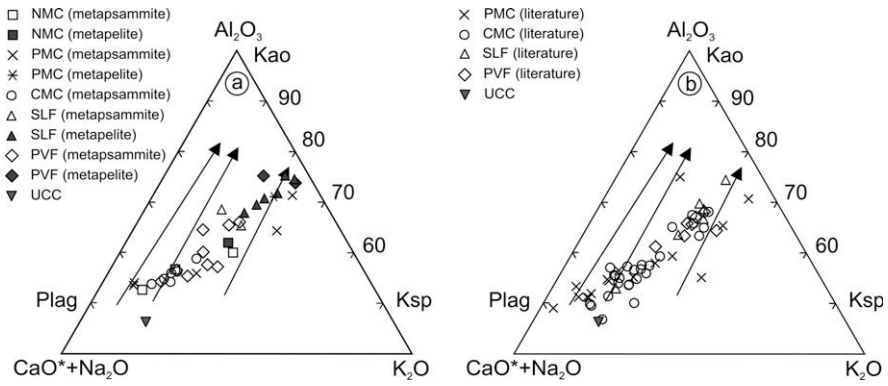

Fig. 4. The chemical index of alteration (CIA) for the metamorphic complexes of the Sierra de San Luis and the Puncoviscana Formation of the Cordillera Oriental (Nesbit and Young, 1982). The arrows represent ideal weathering trends of granite (right-hand side), granodiorite (central arrow) and tonalite (left-hand side). A trend subparallel to the ideal weathering trend is observed for the whole data collection and the individual units which show different starting sources. Plag: Plagioclase, Kao: Kaolinite, Ksp: Potassium feldspar. (a) Samples investigated in this study. (b) Samples taken from Sims et al. (1998), Brogioni (2001), López de Luchi et al. (2003) for the Sierra de San Luis and Zimmermann (2005) for the Puncoviscana Formation.

abundances are 74% SiO_2 and 11.9% Al_2O_3 for the metapsammitic and metapsammopelitic rocks. The metapelitic samples have an average of 60% SiO_2 and 18.4% Al_2O_3. These values are similar to those of the upper continental crust (UCC, Taylor and McLennan, 1981), which has an SiO_2 concentration of 66% and an Al_2O_3 concentration of 15.2%. Exceptions are the samples A13-06 and A19-06 with SiO_2 values of 88% and 84%, and low Al_2O_3 values of 6.2% and 7.4%.

Using the geochemical classification diagram (Fig. 5) of Herron (1988), the metasedimentary rocks of the PVF and the CMC are mostly wackes. Two samples from the PVF plot in the field of shales and two as arkose or lithoarenite, close to the wacke boundary. They are in good agreement to the samples from Zimmermann (2005). Samples from the SLF plot mostly as shales except for A9-01 (lithoarenite) and A12-06 (arkose). Most of the samples from the PMC plot in the arkose or lithoarenite fields except for one metapelite. Two samples of the NMC plot as lithoarenite. The fields defined by the data of Sims et al. (1998), Brogioni (2001) and López de Luchi et al. (2003) cover wider fields in the graph, than the new data, but the tendency for the PMC to be more SiO_2 rich is similar, whereas shales for the CMC do not appear in the present data collection.

The SLF is characterised by SiO_2 concentrations between 56% and 64% except for the arkose and the lithoarenite. The PMC shows one metapelite with an SiO_2 value around 59% and predominant metapsammites with an average of 79% of SiO_2. The NMC is dominated by metapsammites with SiO_2 values of around 77%. The CMC wackes exhibit a narrow range of SiO_2 between 68% contents 74%, whereas the PVF metapelites are characterised by SiO_2 of around 61%. The metawackes are similar to the CMC. If the data set of López de Luchi et al. (2003) is considered, the SiO_2 range is similar for the PVF and the CMC, whereas the PMC and the SLF show a tendency to a more bimodal distribution with rocks of SiO_2 contents lower than 65% or higher than 72%.

The sum of $Fe_2O_{3(t)}$ + MgO for the metapsammitic samples of the PMC, the SLF and the NMC are around or below 5%, which is characteristic for rocks with a quartzose sedimentary or felsic igneous provenance. The CMC and the PVF, however, show an average of 8% (Fig. 6), which is an indication for at least some intermediate igneous provenance (Roser and Korsch, 1988).

The contrasting compatibility of Th and Sc in basic rocks makes the Th/Sc ratio a good tracer for identifying mafic components in clastic materials (Fig. 7) and the maturity of the source area. The limit of 0.8 for the Th/Sc ratio is taken as a reference in the UCC (Taylor and McLennan, 1981; McLennan et al., 1990; McLennan, 2001). As Th is highly incompatible the ratio will be high in rocks derived from the crust and low in rocks with a mantle origin. The samples from the NMC show values between 1.1 and 1.6. In the PMC three samples vary between 1.1 and 1.4 and two show values

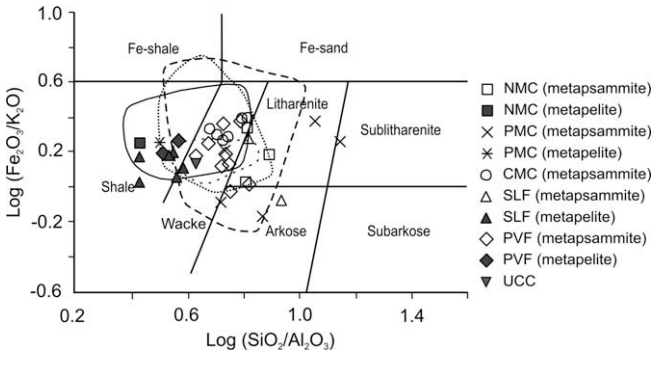

Fig. 5. Chemical classification of the metaclastic rocks in the metamorphic complexes of the Sierra de San Luis and the Puncoviscana Formation of Cordillera Oriental based on the log (Fe_2O_3t/K_2O) vs. log (SiO_2/Al_2O_3) of Herron (1988). Fields correspond to the data of Sims et al. (1998), Brogioni (2001), López de Luchi et al. (2003) and Zimmermann (2005). Conlara Metamorphic Complex: solid line, San Luis Formation: dotted line, Pringles Metamorphic Complex: long dashed line, Puncoviscana Formation: short dashed line.

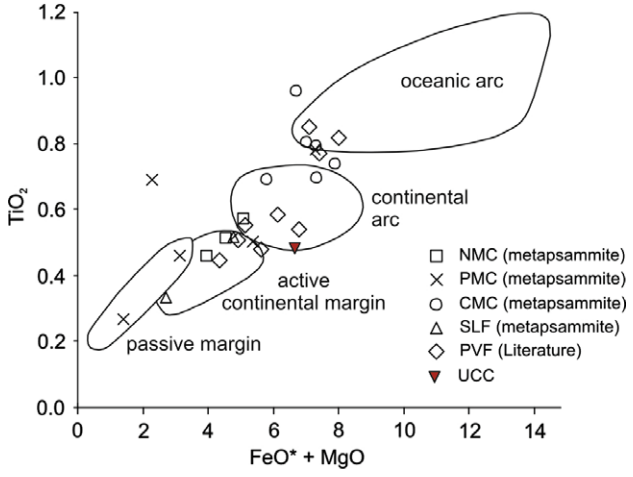

Fig. 6. Tectonic setting discrimination plot based on TiO_2 vs. Fe_2O_{3T} + MgO (Bhatia, 1983) for samples of the metamorphic complexes of the Sierra de San Luis and the Puncoviscana Formation of the Cordillera Oriental.

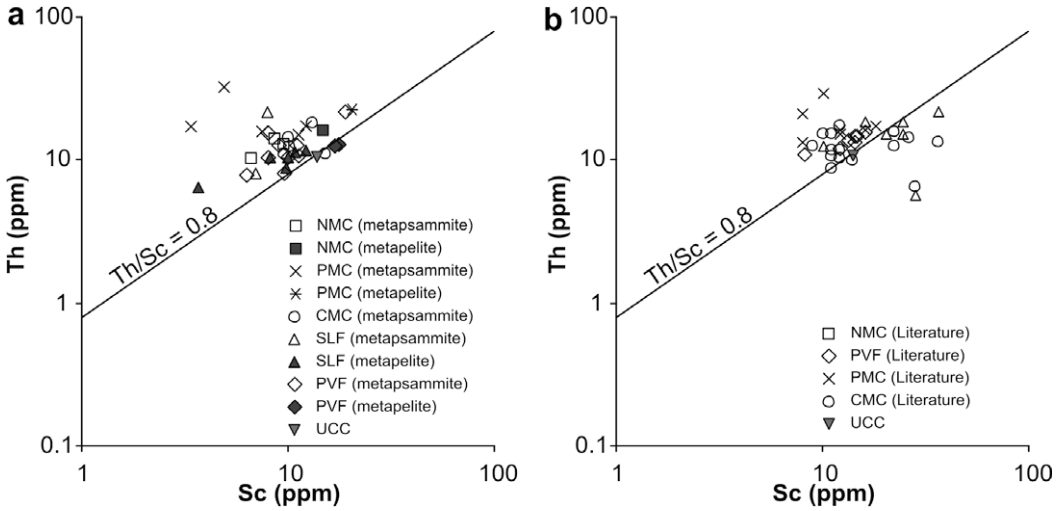

Fig. 7. Source and compositional discrimination plots of Th vs. Sc for samples from the metamorphic complexes of the Sierra de San Luis and the Puncoviscana Formation of the Cordillera Oriental. A Th/Sc value of 0.8 is the lower limit for continental crust (McLennan et al., 1990). (a) Samples analysed in this study. (b) Samples taken from Sims et al. (1998), Brogioni (2001), López de Luchi et al. (2003) for the Sierra de San Luis and Zimmermann (2005) for the Puncoviscana Formation.

of 5.1 and 6.7. The unusually high ratios might be the result of the high SiO_2 contents (84% and 88%). The CMC and the PVF yielded comparable results between 0.7 and 1.4, except for one sample of PVF (A87-06) that shows a value of 1.9. The ratios of the SLF vary between 0.9 and 1.7 for the metapelites and between 1.1 and 2.6 for the metapsammitic rocks. Three samples from the whole collection are slightly below the limit of 0.8. A9-06 is a low-grade metapsammite, located in the northwest of the CMC (Fig. 3) and the other two samples (A85-06, A86-06), located west of the city of Tucumán, are metapelites of the PVF that exhibit SiO_2/Al_2O_3 ratios around 4 (Fig. 2). Only the rhyolitic sample (A17-06) from the SLF shows a value far below the limit of the UCC of 0.3.

Mafic rocks that may indicate a suture zone between different terranes (ophiolites) can be identified by Cr/V ratios >8 and Y/Ni ratios <0.5 (Hiscott, 1984; Dinelli et al., 1999). High Cr/V values monitor the enrichment of chromite over ferromagnesian minerals, whereas the Y/Ni ratio compares a ferromagnesian trace element (Ni) with Y, which is used as a proxy for the heavy REE (McLennan et al., 1993). The samples are characterised by Cr/V ratios between 0.7 and 1.3 (Fig. 8) and Y/Ni ratios between 0.5 and 3.5 (Fig. 9). The more pelitic samples from the SLF show lower values for Y/Ni, however, when the SiO_2 is around 80%, the PMC shows higher values than both the CMC and PVF.

Chondrite normalised REE plots are rather uniform (Fig. 10). The average concentration of total REE is 143 ppm for the PVF, 171 ppm for the NMC, 200 ppm for the PMC, 214 ppm for the CMC and 117 ppm for the SLF. Sample A96-06 of the PVF with 346 ppm, located close to the Cafayate pluton was not taken into the calculation of the mean value. The average concentration of the UCC and the post-Archaean average Australian shale (PAAS) are 148 ppm and 181 ppm (Nance and Taylor, 1976; Taylor and McLennan, 1981). Compared to these values the PVF is similar to the UCC, whereas the SLF is depleted and the rest is enriched in the total amount of REE. If the PAAS is considered, the PMC and the CMC are enriched and the rest depleted. The $(La/Yb)_N$ ratios vary between 6 and 9 for the SLF, 6–10 for the NMC and 6–9 for the PVF. The PMC shows bimodal ratios of 7–9 and 13 (A14-06 and A15-06 from the central part of the complex). This is also observable in the CMC, where five samples have values of 7–10, but one rock (A23-01, located in the central part of the CMC) has an

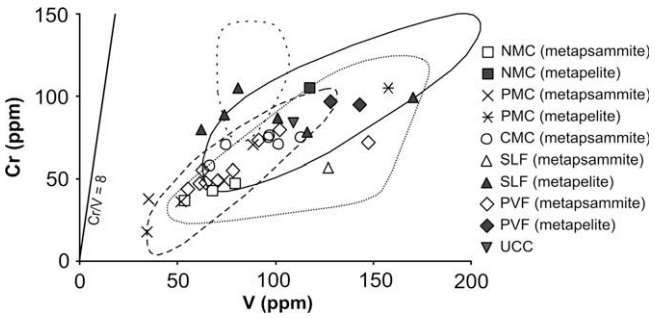

Fig. 8. Source and compositional discrimination plots of Cr vs. V for samples of the metamorphic complexes of the Sierra de San Luis and the Puncoviscana Formation of the Cordillera Oriental. Only seven samples from the SLF are plotted in the diagram, because Cr was below the detection limit in one sample (A12-06). The fields correspond to the data of Sims et al. (1998), Brogioni (2001), López de Luchi et al. (2003) and Zimmermann (2005). Conlara Metamorphic Complex: solid line, San Luis Formation: dotted line, Pringles Metamorphic Complex: long dashed line, Puncoviscana Formation: short dashed line.

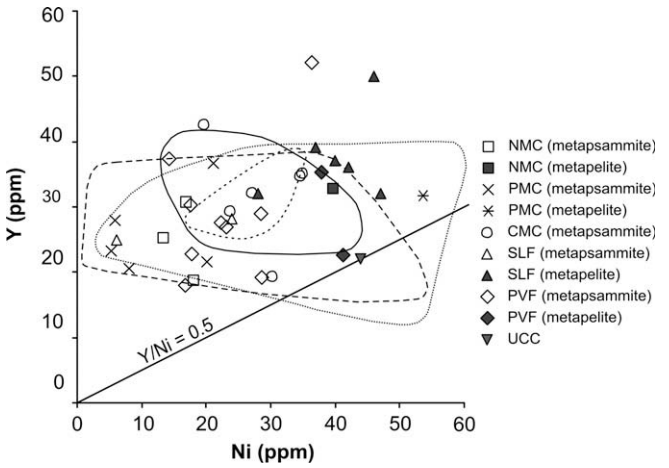

Fig. 9. Source and compositional discrimination plots of Y vs. Ni (McLennan et al. 1993) for samples of the metamorphic complexes of the Sierra de San Luis and the Puncoviscana Formation of the Cordillera Oriental. Y/Ni ratios lower than 0.5 indicate mafic sources. The fields correspond to the data of Sims et al. (1998), Brogioni (2001), López de Luchi et al. (2003) and Zimmermann (2005). Conlara Metamorphic Complex: solid line, San Luis Formation: dotted line, Pringles Metamorphic Complex: long dashed line, Puncoviscana Formation: short dashed line.

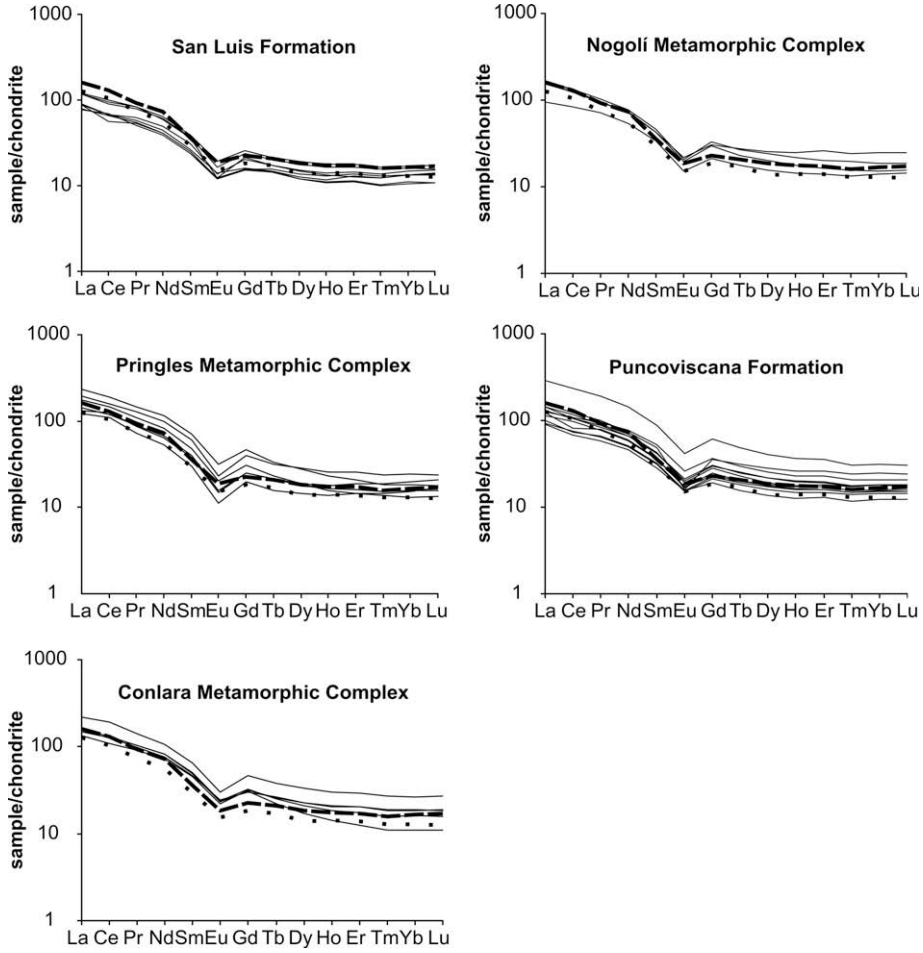

Fig. 10. Chondrite normalised REE patterns (Taylor and McLennan, 1985) for samples of the metamorphic complexes of the Sierra de San Luis and the Puncoviscana Formation of the Cordillera Oriental. The dashed lines represent the post-Archaean average Australian shale (PAAS) and the dotted line symbolises the upper continental crust (UCC) as defined by McLennan (1989).

elevated ratio of 14 (Fig. 3). The analysed rocks exhibit a moderate to significant Eu/Eu^* anomaly with average values between 0.5 and 0.6 for all units. These ratios point to typical UCC sources (Taylor and McLennan, 1981; McLennan et al., 1990).

Under surface conditions Ce^{4+} is less mobile than the other LREEs that occur as triple positively charged ions. Therefore, the Ce/Ce^* anomaly is considered to be a proxy for the depletion of LREEs under surface conditions (e.g. McLennan, 1989). High Ce/Ce^* anomalies generally go along with a depletion of the LREE, which results in low ΣREE. The Ce/Ce^* anomalies are all ~1 for the samples from the Sierra de San Luis (0.95–1.12), except for the SiO_2-rich samples A13-06 and A19-06 (1.21–1.23) from the PMC. A significant depletion of the LREE under surface processes is not indicated, except for A13-06 and A19-06 (cf. Fig. 10), which provide the lowest total concentration of REE and the lowest slope for La_N/Yb_N in the PMC. This agrees with a relatively restricted range of $^{147}Sm/^{144}Nd$, indicating no significant fractionation within the REE.

The Zr/Sc ratio (Fig. 11) varies between 8 and 27 for the PVF, between 14 and 32 for the NMC, similar to the CMC (12–29) and close to the SLF showing values of 13–20 and 27 and 38 for the samples A12-06 and A30-01, respectively. The PMC has the broadest distribution of the Zr/Sc ratios between 11 and 223. The two highest values, pointing to higher crustal reworking, originate from samples with very high SiO_2 contents around 85% (A13-06, A19-06). These values for the Zr/Sc ratio may result from the presence of a few heavy minerals, which can influence the sample to a greater extent compared to a pelite. A19-06 has an extremely high Zr/Sc value of over 200, but since the Zr content is extremely high (760 ppm), this result is difficult to evaluate. A13-06 exhibits a very high Th/Sc

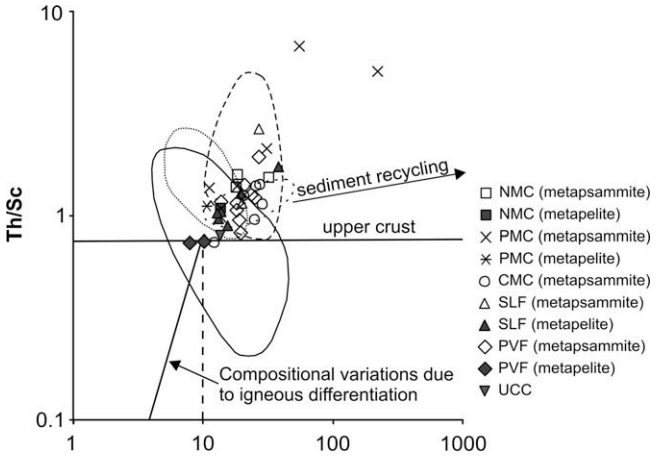

Fig. 11. Provenance and recycling discrimination plot of Th/Sc vs. Zr/Sc (McLennan et al., 1990) for samples of the metamorphic complexes of the Sierra de San Luis and the Puncoviscana Formation of the Cordillera Oriental. Th/Sc >0.8 reflects the provenance of the samples from the upper continental crust, and Zr/Sc is a proxy for sediment recycling, as Zr mostly comes from zircons that are highly resistant to weathering. The samples overlap each other, but some samples of the PMC are located towards higher values of Zr/Sc, thus indicating a higher degree of recycling.

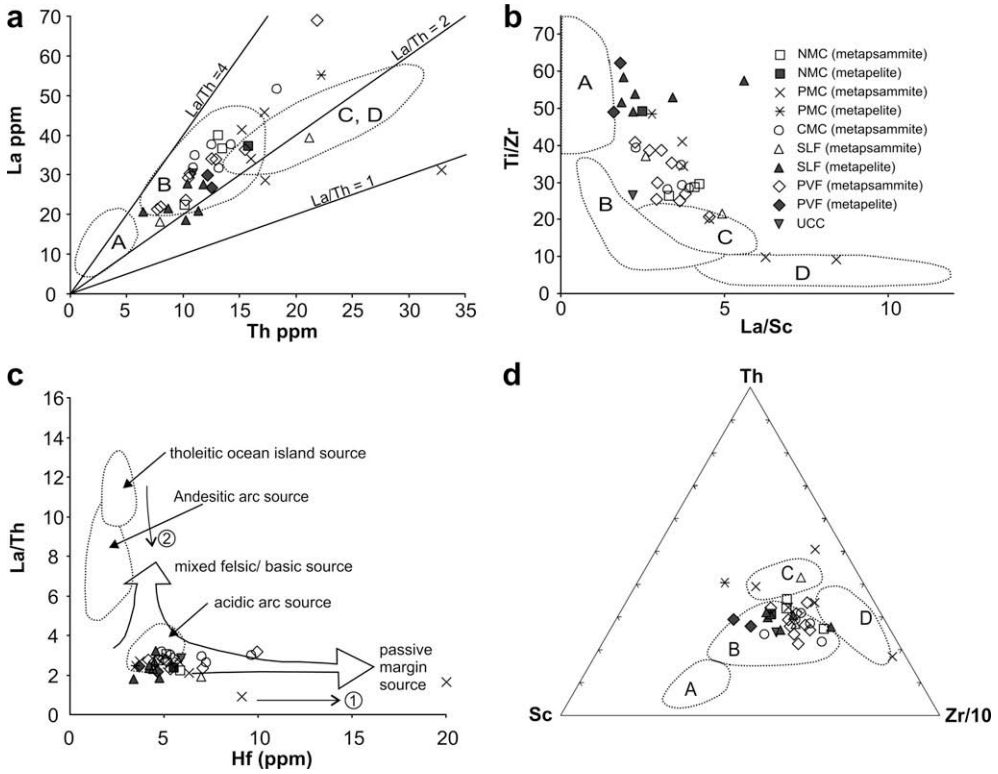

Fig. 12. Tectonic setting discrimination plots based on trace elements for samples of the metamorphic complexes of the Sierra de San Luis and the Puncoviscana Formation of the Cordillera Oriental. (a), (b), and (d) after Bhatia and Crook (1986), (c) after Floyd and Leveridge (1987). Fields are: A – oceanic island-arc, B – continental island-arc, C – active continental margin, D – passive continental margin. Most of the samples plot in the continental island-arc field. See text for comments.

ratio of 6.7 and a value of 55 for Zr/Sc. Both samples are far outside the range of all other metaclastic material.

In the TiO_2 vs. $Fe_2O_{3(tot)}$ + MgO diagram (Bhatia, 1983), the samples mostly plot in the fields of continental island-arc or active continental margin, except for the PMC that is biased toward the passive margin field (Fig. 6). The La/Th value behaves concordantly during sedimentary processes, therefore it would be characteristic for the source (Bhatia and Crook, 1986). Ti and Sc display volcanic/mantle input, whereas Zr and La monitor the degree of recycling (Bhatia and Crook, 1986). Consequently, the Ti/Zr vs. La/Sc plot would reflect the contribution of magmatic vs. recycled sources and the La/Sc value, the felsic against the mafic magmatic input, i.e. the involvement of the input from a passive continental margin vs. the input from an oceanic island-arc source.

La/Th vs. Hf plots are used for discriminating the tectonic setting. Hf displays the degree of recycling and La/Th is controlled by the mafic–felsic composition of the magmas, as Th is incompatible and thus enriched in more evolved magmas. In the plots of Fig. 12a–d the samples mostly plot in the field of a continental island-arc, or in the active continental margin field, except for the PMC that always exhibits a trend to more recycled sources. Most of the samples plot in an area of La/Th ratios between 2 and 4. Some samples of the PMC and the SLF define an array with lower La/Th (Fig. 12a), whereas the rest of the samples plot along a La/Th trend of about 3.

The group of samples from the PMC with lower La/Th values shows relatively higher La/Sc and a trend to higher Hf contents. The sources for them are either more felsic/recycled and exhibit a more defined trend towards continental arc or even passive margins in tectonic diagrams. The rest of the samples from the PMC also show higher La/Sc ratios at a given Ti/Zr value, but no clear Hf enrichment nor a location towards continental margins. The SLF exhibits low values for the La/Th ratio, but the samples still plots in the field of continental island-arc. This is similar to the rest of the tectonic setting diagrams, except for the La/Sc vs. Ti/Zr plot, in which the metapelitic samples from all units plot very close to or in the continental island-arc field. Since this diagram was originally constructed for greywackes, it is possible that it is not appropriate for (meta) pelites.

The data for the NMC, the CMC and the PVF mostly plot in the continental island-arc field. However, La/Sc quotients are higher than the normal values for the rocks of this tectonic setting (Fig. 12b), and the Hf content is comparable to the UCC, which suggests no strong influence from old crustal material that would be characteristic for a passive margin.

4.3. Whole rock Sm–Nd results

The T_{DM} ages were calculated based on the model of Goldstein et al. (1984) that assumes a linear evolution of the isotopic composition. Previously published data was, if calculated with another model, recalculated with the model of Goldstein et al. (1984). The εNd data of all analysed samples were back calculated to 540 Ma, which is the best approximation on the timing of their deposition (Sims et al., 1998; Söllner et al., 2000; Steenken et al., 2006; Adams et al., 2006), although the sedimentation age of the PMC might be younger. Calculations for the $\varepsilon Nd_{(540\ Ma)}$ and T_{DM} data are shown in Figs. 13 and 14. All the samples have $^{147}Sm/^{144}Nd$ values ranging from 0.110 to 0.126 (Table 2). This relatively narrow range of $^{147}Sm/^{144}Nd$ values indicates only a slight differentiation of the Sm/Nd ratio during the sedimentation and/or at the time of emplacement into the crust, and little fractionation of the REE during the exogenic processes (Jahn and Condie, 1995). This is also reflected by the $f_{Sm/Nd}$ that has typical values between −0.34 and −0.47 for the continental crust (Goldstein et al., 1984). All analysed samples are within this range.

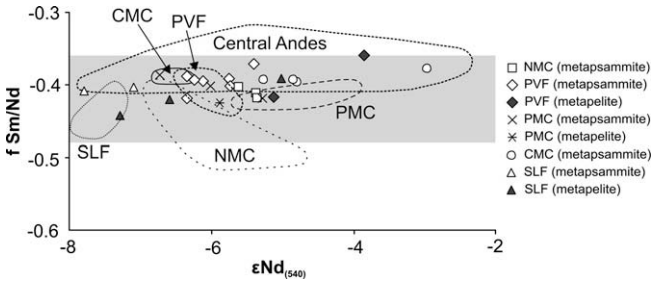

Fig. 13. Plot of $f_{Sm/Nd}$ vs. $\varepsilon Nd_{(540\ Ma)}$ for samples of the metamorphic complexes of the Sierra de San Luis and the Puncoviscana Formation of the Cordillera Oriental. The fields for the other major units are added for comparison. Most samples scatter around εNd values of −5 and −6.5. Samples from the Arequipa–Antofalla craton (Central Andes) cover the complete spread of the $\varepsilon Nd_{(540\ Ma)}$. Four of the five samples of the San Luis Formation show a less radiogenic $\varepsilon Nd_{(540\ Ma)}$. Data from the central Andes from Lucassen et al. (2000), all fields for the Sierra de San Luis from Steenken et al. (2004) and for the Puncoviscana Formation from Bock et al. (2000). The grey field represents the $f_{Sm/Nd}$ limits for the continental crust (Goldstein et al., 1984). Conlara Metamorphic Complex: solid line, San Luis Formation: dotted line, Pringles Metamorphic Complex: long dashed line, Puncoviscana Formation: short dashed line, Nogolí Metamorphic Complex: dashed-dotted line.

The PVF (Table 2) shows $\varepsilon Nd_{(540\ Ma)}$ ratios between −6.3 and −3.9 (n = 9) and T_{DM} ages between 1.80 and 1.63 Ga. Similar values were obtained by Bock et al. (2000). The very low-grade metapelitic rocks A85-06 and A86-06, taken immediately to the west of the city of Tucumán, exhibit almost similar T_{DM} ages of 1.66 and 1.63 Ga and $\varepsilon Nd_{(540\ Ma)}$ values of −5.1 and −3.9. The T_{DM} ages from these samples differ from the rest of the PVF, where crustal residence times between 1.80 and 1.72 Ga are recognised. In addition, the $\varepsilon Nd_{(540\ Ma)}$ data from the samples near Tucumán are higher than the rest of the analysed samples, which give values between −6.3 and −5.4.

In the Sierra de San Luis, the rocks of the NMC show T_{DM} ages between 1.70 and 1.64 Ga, and $\varepsilon Nd_{(540\ Ma)}$ data between −5.6 and −5.3. In the PMC, the data varies from 1.83–1.64 Ga and $\varepsilon Nd_{(540\ Ma)}$ between −6.7 and −5.3. A13-06 (SiO_2 87%) yields the oldest T_{DM} of 1.83 Ga, whereas A14-06 and A15-06 are significantly younger (1.64 Ga and 1.67 Ga). A18-06 (SiO_2 84%) exhibits a T_{DM} age of 1.74 Ga. The youngest model ages were found in the CMC with T_{DM} ages of 1.69–1.65 Ga and $\varepsilon Nd_{(540\ Ma)}$ data between −5.3 and −4.8. Sample A61-05 shows the youngest T_{DM} age so far found in the metaclastic rocks, with an age of 1.54 Ga and an $\varepsilon Nd_{(540\ Ma)}$ value of −3.0. Four samples from the SLF yielded a narrow spectrum of $\varepsilon Nd_{(540\ Ma)}$ values between −7.8 and −6.6 and T_{DM} ages between 1.86 and 1.74 Ga. Sample A30-01 shows a slightly younger T_{DM} of 1.68 Ga and an elevated $\varepsilon Nd_{(540\ Ma)}$ value of −5.0 (Table 2).

These results are in accordance with most of the previous Nd isotope analyses of the Sierra de San Luis (Steenken et al., 2004), except for the CMC. This unit exhibits a trend to higher εNd values and a younger T_{DM} age, which differs from the results for two banded schists obtained by Steenken et al. (2004) that yielded an older T_{DM} age of 1.8 Ga and $\varepsilon Nd_{(540\ Ma)}$ values between −6 and −7.

4.4. Whole rock Pb–Pb results

The Pb isotopic system has already been used in the southwestern part of South America by several authors (e.g. Aitcheson et al., 1995; Kay et al., 1996; Tosdal, 1996; Bock et al., 2000; Loewy et al., 2004; Schwartz and Gromet, 2004) to discriminate between different basement domains. In the case of a basin, fed from a uniform reservoir or a mixture of different reservoirs, the Pb isotope ratios should result in a linear trend. The Pb ratios represent the average Pb isotopic composition of the metasedimentary source rocks. The present day Pb values of this dataset define a linear trend in the $^{207}Pb/^{204}Pb$ vs. $^{206}Pb/^{204}Pb$ (Fig. 15) and the $^{208}Pb/^{204}Pb$ vs. $^{206}Pb/^{204}Pb$ (Fig 16) diagrams. This linear trend results from the additional production of Pb from U and Th. The whole rock data (Table 3) cover an interval of 18.35–19.84 for the $^{206}Pb/^{204}Pb$ ratio, 15.63–15.89 for the $^{207}Pb/^{204}Pb$ value and 38.59–40.17 for the $^{208}Pb/^{204}Pb$ quotient (Figs. 15 and 16). Sample A10-06 from the CMC lies outside the plotting field of the rest of the data collection. This rock was taken near a tonalite pluton. Nevertheless, a modification of the data is not assumed. The isotopic ratios are high, but the sample plots in the linear array of the trend of the other samples. The reason for the high values might derive from the additional production of Pb from U and Th. The contents of these elements are not unusually high (3.5 ppm U and 18.3 ppm Th), but have a big effect because of the relatively low Pb concentration (8.5 ppm). Two other samples (A12-06 and A88-06) show elevated $^{207}Pb/^{204}Pb$ values and are above the common trend.

The NMC exhibits a very restricted range for $^{207}Pb/^{204}Pb$ ratios, whereas the rest shows a wider range.

Since ^{207}Pb is generated by the decay of short-lived ^{235}U, differences in present day $^{207}Pb/^{204}Pb$ ratios must reflect ancient differentiation events. The more recent the differentiation is, the smaller the eventual difference in $^{207}Pb/^{204}Pb$ values, given the increasing scarcity of the parent ^{235}U isotope. Another peculiarity can be found in the $^{208}Pb/^{204}Pb$ vs. $^{206}Pb/^{204}Pb$ diagram (Fig. 16), in which the samples of the PMC are slightly above the linear array for the rest of the samples.

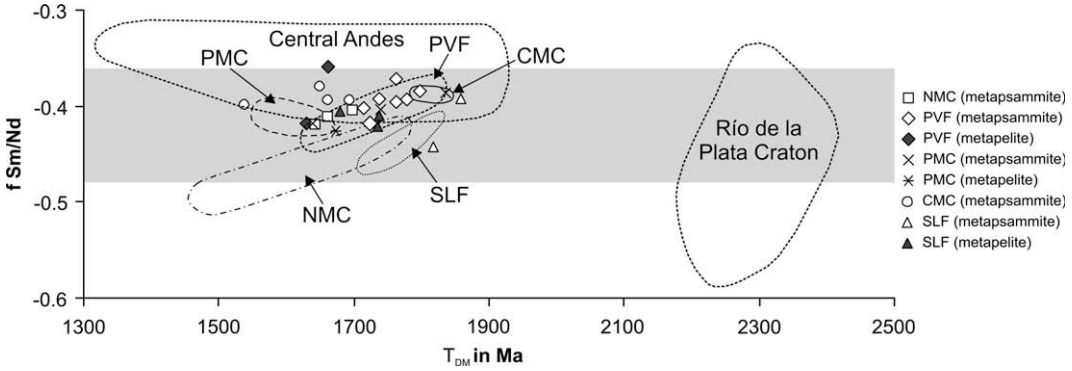

Fig. 14. Plot of $f_{Sm/Nd}$ vs. T_{DM} ages for samples of the metamorphic complexes of the Sierra de San Luis and the Puncoviscana Formation of the Cordillera Oriental. The samples and calculation are the same as in Fig. 13, including the horizontal grey field. Data from the central Andes is from Lucassen et al. (2000), for the Sierra de San Luis from Steenken et al. (2004), for the Puncoviscana Formation from Bock et al. (2000) and for the Río de la Plata from Iacumín et al. (2001) and Pankhurst et al. (2003). T_{DM} ages are far apart from those of the Rio de la Plata craton. See text for comments. San Luis Formation: dotted line, Pringles Metamorphic Complex: long dashed line, Puncoviscana Formation: short dashed line, Nogolí Metamorphic Complex: dashed-dotted line.

Table 2
Sm/Nd data for metasediments from the different domains of the Sierra de San Luis and the Puncoviscana Formation of the Cordillera Oriental. T_{DM} ages are calculated after the model of Goldstein et al. (1984), with $^{143}Nd/^{144}Nd$ of 0.513151 and $^{147}Sm/^{144}Nd$ of 0.214. The fractionation index $f_{Sm/Nd}$ is calculated in the following way: $f_{Sm/Nd} = [(^{147}Sm/^{144}Nd)_{sample}/(^{147}Sm/^{144}Nd)_{CHUR}] - 1$, using $(^{147}Sm/^{144}Nd)_{CHUR} = 0.1967$ of DePaolo and Wasserburg (1976). The Sm and Nd concentrations were measured with the TIMS.

Sample	Sm (ppm)	Nd (ppm)	$^{147}Sm/^{144}Nd$	$^{143}Nd/^{144}Nd$	±2se abs	T_{DM} (Ga)	$eps_{(0)}$	$eps_{(540)}$	$f_{(Sm/Nd)}$
Nogoli Metamorphic Complex									
A7-06	5.932	30.613	0.117	0.512069	0.000014	1.70	−11.1	−5.6	−0.40
A8-06	6.239	32.640	0.116	0.512076	0.000014	1.66	−11.0	−5.4	−0.41
A16-06	6.514	34.466	0.114	0.512073	0.000011	1.64	−11.0	−5.3	−0.42
Pringles Metamorphic Complex									
A13-06	3.608	18.090	0.121	0.512024	0.000010	1.83	−12.0	−6.7	−0.39
A14-06	7.318	38.692	0.114	0.512077	0.000019	1.64	−11.0	−5.3	−0.42
A15-06	9.854	52.718	0.113	0.512040	0.000009	1.67	−11.7	−5.9	−0.43
A18-06	5.775	29.678	0.118	0.512050	0.000108	1.74	−11.5	−6.0	−0.40
Conlara Metamorphic Complex									
A61-05	7.859	38.857	0.122	0.512223	0.000014	1.54	−8.1	−3.0	−0.38
A73-05	7.364	37.539	0.118	0.512117	0.000014	1.65	−10.2	−4.8	−0.40
A9-06	5.892	29.871	0.119	0.512116	0.000022	1.66	−10.2	−4.8	−0.39
A10-06	9.368	47.522	0.119	0.512094	0.000013	1.69	−10.6	−5.3	−0.39
San Luis Formation									
A7-01	9.221	50.831	0.110	0.511958	0.000016	1.74	−13.3	−7.3	−0.44
A9-01	5.553	28.922	0.116	0.511954	0.000008	1.86	−13.4	−7.8	−0.41
A17-01	6.411	34.053	0.113	0.512007	0.000007	1.74	−12.3	−6.6	−0.42
A30-01	5.780	29.241	0.119	0.512108	0.000014	1.68	−10.3	−5.0	−0.39
A12-06	4.965	25.607	0.117	0.511994	0.000012	1.82	−12.6	−7.1	−0.40
Puncoviscana Formation									
A85-06	6.453	34.098	0.114	0.512084	0.000013	1.63	−10.8	−5.1	−0.42
A86-06	7.621	36.553	0.126	0.512190	0.000032	1.66	−8.7	−3.9	−0.36
A87-06	6.155	30.114	0.124	0.512103	0.000118	1.76	−10.4	−5.4	−0.37
A88-06	5.475	27.822	0.119	0.512050	0.000011	1.76	−11.5	−6.1	−0.40
A90-06	6.284	31.868	0.119	0.512044	0.000012	1.78	−11.6	−6.2	−0.39
A91-06	5.391	27.274	0.120	0.512071	0.000016	1.74	−11.1	−5.7	−0.39
A93-06	5.399	28.543	0.114	0.512022	0.000016	1.72	−12.0	−6.3	−0.42
A94-06	5.604	28.170	0.120	0.512043	0.000021	1.80	−11.6	−6.3	−0.39
A97-06	7.152	36.734	0.118	0.512065	0.000016	1.72	−11.2	−5.7	−0.40

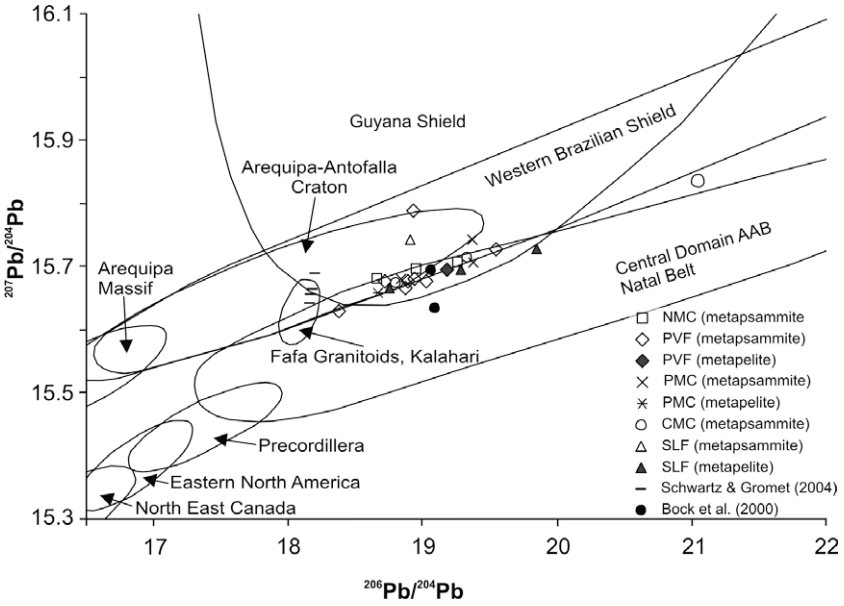

Fig. 15. $^{207}Pb/^{204}Pb$ vs. $^{206}Pb/^{204}Pb$ isotopic correlation diagram (present day Pb) for the studied areas. The fields for the different basement domains are taken from Tosdal (1996) and Schwartz and Gromet (2004). The data plots in the vicinity of the results from Bock et al. (2000) and Schwartz and Gromet (2004). Both groups used metasedimentary rocks for their analyses.

The interval of whole rock Pb data overlaps the compositional data for western Gondwana as defined by Loewy et al. (2004 and references therein). The best overlap is observed with the samples from Quebrada Choja or Belén (Central Domain Arequipa–Antofalla basement) in the uranogenic and in the thorogenic plot.

4.5. Detrital zircon geochronology: U–Pb SHRIMP dating

SHRIMP U/Pb zircon analyses were performed on four samples of the Sierra de San Luis. Two samples belong to the northern section of the NMC, whereas the other two were taken from the CMC

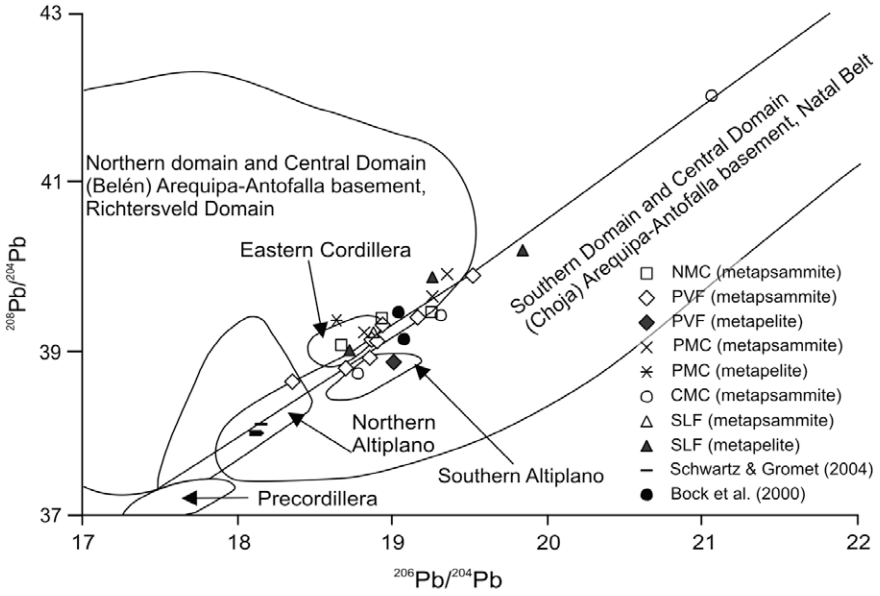

Fig. 16. Isotopic correlation diagram for $^{208}Pb/^{204}Pb$ vs. $^{206}Pb/^{204}Pb$ (present day Pb) with Pb domains of South America after Aitcheson et al. (1995), Kay et al. (1996), Loewy et al. (2003, 2004 and references therein).

Table 3
Whole rock Pb isotopic data for the different domains of the Sierra de San Luis and the Puncoviscana Formation of the Cordillera Oriental.

Sample	$^{206}Pb/^{204}Pb$	±2s	$^{207}Pb/^{204}Pb$	±2s	$^{208}Pb/^{204}Pb$	±2s	$^{207}Pb/^{206}Pb$	±2s	Pb l F	±2s
Conlara Metamorphic Complex										
A61-05	19.310	0.012	15.716	0.011	39.368	0.033	0.8139	0.0002	2.0387	0.0007
A9-06	18.785	0.009	15.676	0.010	38.671	0.029	0.8345	0.0002	2.0586	0.0007
A10-06	21.061	0.014	15.835	0.012	42.013	0.039	0.7519	0.0002	1.9948	0.0010
Pringles Metamorphic Complex										
A13-06	19.352	0.012	15.743	0.012	39.878	0.034	0.8135	0.0002	2.0607	0.0007
A14-06	18.816	0.014	15.683	0.013	39.185	0.039	0.8335	0.0002	2.0825	0.0011
A15-06	18.642	0.012	15.659	0.012	39.314	0.035	0.8400	0.0002	2.1089	0.0009
A18-06	19.259	0.009	15.712	0.010	39.613	0.031	0.8158	0.0002	2.0568	0.0009
Nogoli Metamorphic Complex										
A7-06	19.254	0.012	15.706	0.011	39.402	0.033	0.8157	0.0002	2.0465	0.0007
A8-06	18.941	0.022	15.698	0.020	39.343	0.053	0.8288	0.0003	2.0771	0.0010
A16-06	18.673	0.008	15.679	0.009	39.009	0.029	0.8396	0.0002	2.0890	0.0008
San Luis Formation										
A11-01	19.840	0.013	15.731	0.012	40.171	0.035	0.7929	0.0002	2.0248	0.0007
A32-01	18.726	0.010	15.669	0.010	38.968	0.031	0.8367	0.0002	2.0810	0.0008
A34-01	19.262	0.009	15.696	0.010	39.840	0.031	0.8149	0.0002	2.0684	0.0008
A12-06	18.880	0.010	15.744	0.011	39.177	0.032	0.8339	0.0002	2.0750	0.0008
Puncoviscana Formation										
A86-06	19.012	0.009	15.679	0.009	38.822	0.029	0.8247	0.0002	2.0420	0.0007
A87-06	19.158	0.012	15.695	0.011	39.358	0.033	0.8193	0.0002	2.0544	0.0007
A88-06	18.931	0.014	15.763	0.013	39.261	0.037	0.8327	0.0002	2.0739	0.0007
A89-06	18.866	0.010	15.680	0.010	39.086	0.031	0.8311	0.0002	2.0718	0.0007
A91-06	18.903	0.008	15.679	0.009	39.078	0.028	0.8295	0.0002	2.0674	0.0007
A93-06	18.352	0.009	15.631	0.010	38.588	0.029	0.8517	0.0002	2.1027	0.0007
A94-06	18.700	0.018	15.678	0.016	38.741	0.044	0.8384	0.0002	2.0718	0.0009
A96-06	19.520	0.013	15.725	0.012	39.852	0.036	0.8056	0.0002	2.0416	0.0008
A97-06	18.851	0.010	15.673	0.010	38.873	0.030	0.8314	0.0002	2.0621	0.0008

and the SLF. All ages discussed here are $^{206}Pb/^{238}U$ ages, if not named differently.

The samples A7-06 and A8-06 were taken from the same outcrop along the road between La Carolina and San Francisco del Monte de Oro crossing the northern portion of the NMC and will be interpreted together. Small quartz and/or quartz–plagioclase veins crosscut the sample. Both represent grey medium-grained metapsammitic gneisses with quartz, biotite, plagioclase and muscovite as major constituents. The accessory minerals are apatite and zircon in both samples. A7-06 shows some clinozoisite. The samples correspond to the Ms–Bt/Bt–Ms gneisses described by von Gosen and Prozzi (1998).

The zircons show many different kinds of shapes, from long-prismatic, to short-prismatic and different degrees of rounded forms. All dated zircons show a magmatic zoning in large parts of the grains. Although the long prismatic grains show less pronounced zoning, they still exhibit a complex history by inherited cores and metamorphic overgrowth. Inherited cores are identified

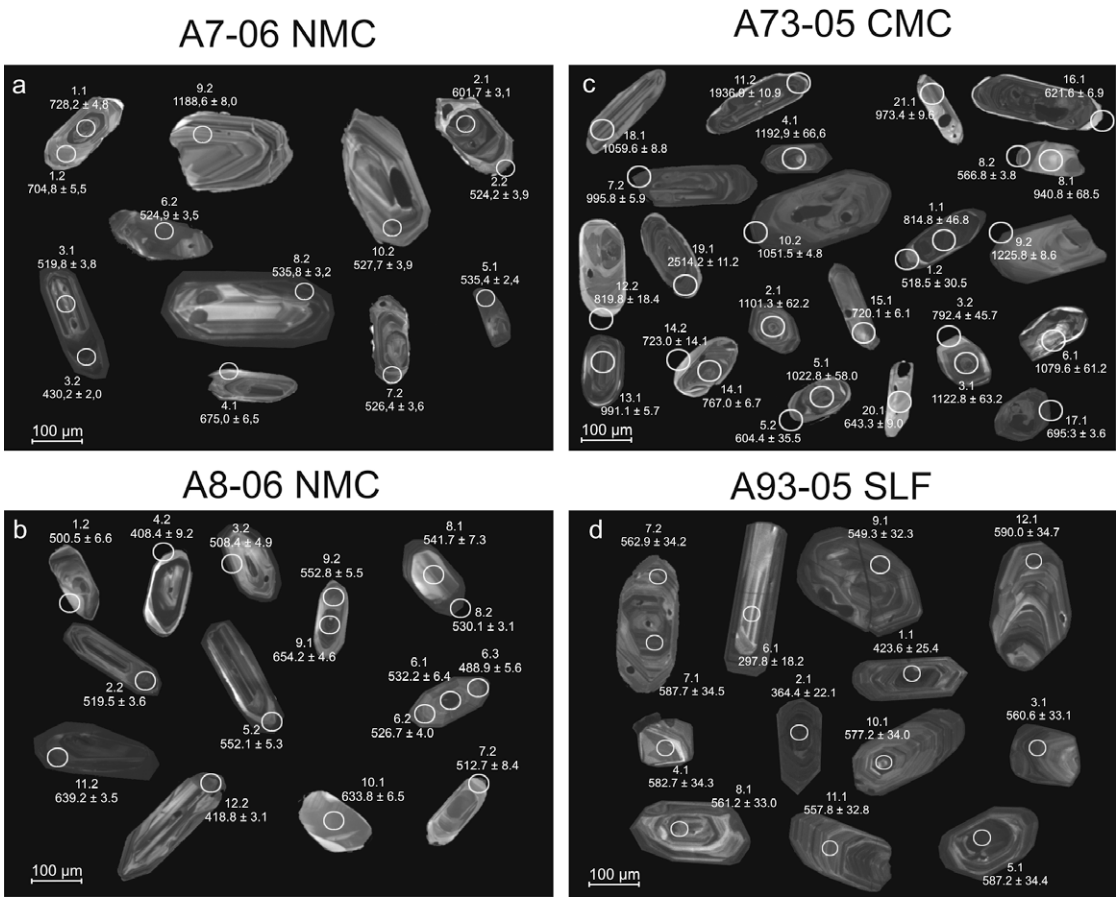

Fig. 17. Cathodoluminescence images of the analysed zircons including measurement spots, ages and errors calculated for the $^{206}Pb/^{238}U$ ratios. Samples: (a) A7-06, (b) A8-06, (c) A73-05 and (d) A93-05.

in only a few zircon grains (Fig. 17a and b). Twenty-nine SHRIMP analyses on 22 grains were done in order to reveal the provenance and the metamorphic history of the NMC. All but three spots yielded Th/U ratios in a range from 0.16 to 1.05 (Table 4), indicating derivation from an igneous provenance. Three analyses show Th/U values between 0.10 and 0.03 that correspond to metamorphic growth. Ten of the analysed spots are highly discordant (more than 20%), these ages were omitted. Two of the 18 samples remaining show Famatinian ages (489 Ma and 501 Ma), eleven yield Pampean ages between 553 and 520 Ma, four show ages corresponding to the Brasiliano orogeny between 730 Ma and 600 Ma and one age of 1190 Ma belongs to a Grenvillian event. Nine of the eleven Pampean ages give a weighted average of 528.5 ± 4.8 Ma, neglecting the two oldest ages of 552 Ma and 553 Ma.

Sample A73-05 is a banded schist from the central part of the CMC. The collected zircons are sub-rounded to rounded with a complex growth history. About 50% are short-prismatic to oblate, the other 50% are long-prismatic. Some zircons show older, rounded cores and at least two further episodes of growth (Fig. 17c). Most of the Th/U ratios are above 0.1. From this sample 26 ages were calculated from 21 grains, starting with a discordant age of 519 Ma, which exhibits a $^{206}Pb/^{207}Pb$ age of 581 ± 52 Ma. The youngest age cluster can be found between 820 Ma and 570 Ma ($n = 12$). These ages correspond to rims of bigger grains and the centre of two prismatic zircons. The oldest analysis points cluster between 1225 Ma and 940 Ma ($n = 12$), which is typical of Grenvillian ages. These values correspond to both cores and rims. Two analyses point to a Palaeoproterozoic source (Table 4). The common ^{206}Pb is about 2% and 2.5% in three cases, reflected by the larger errors for the apparent ages.

Sample A93-05 from the SLF contains short-prismatic to long-prismatic zircons. The Th/U ratios are above 0.49 indicating a magmatic source. The grains often show a magmatic zoning in the outer parts, but the central parts can also be single coloured under cathodoluminescence. This could point to an older core or to a homogeneous magma chamber in the earliest stage of crystallisation. Thirteen ages have been calculated on twelve grains, resulting in three $^{206}Pb/^{238}U$ ages of 423 Ma or younger, with Palaeoproterozoic $^{207}Pb/^{206}Pb$ ages. These young grains plot very discordantly. The other 10 $^{206}Pb/^{238}U$ ages are between 590 and 540 Ma (Table 4). The age spectrum of these grains is relatively narrow and the striking difference to all other samples is the fact that one geological event at 569 ± 20 Ma (MSWD = 3.4) is recorded by these grains. There are no zircons older than 590 Ma and the Palaeoproterozoic and Archaean $^{207}Pb/^{206}Pb$ ages are doubtful due to their extremely high discordance. A core and a rim from one grain resulted in an age of 588 Ma for the core and 563 Ma for the rim.

5. Discussion

5.1. Influence of weathering, sorting and alteration

The effects of variable degrees of weathering in the source area would result in a relative depletion of alkali and alkaline earth elements and in an enrichment of the Al_2O_3 and TiO_2 concentration in the resulting terrigenous sedimentary rocks (Nesbit et al., 1980; Grandstaff et al., 1986; Harnois, 1988). The chemical index of alteration (CIA) for the sample collection varies between 53 and 85, with an average for the metapsammitic rocks of 59 ($n = 25$),

Table 4
SHRIMP zircon data for samples from the Nogolí Metamorphic Complex, banded schist of the Conlara Metamorphic Complex and a phyllite of the San Luis Formation. See Fig. 3 for location.

Grain/Spot						Ages (Ma)				Radiogenic ratios						
	$^{206}Pb_c$	U (ppm)	Th (ppm)	$^{232}Th/^{238}U$	^{206}Pb (ppm)	$^{206}Pb/^{238}U$	±Ma	$^{207}Pb/^{206}Pb$	±Ma	$^{207}Pb/^{206}Pb$	±(%)	$^{207}Pb/^{235}U$	±(%)	$^{206}Pb/^{238}U$	±(%)	% Disc.
A7-06 Nogoli Metamorphic Complex																
3.2	1.02	1101	171	0.16	66.0	430.2	2.0	631	63	.0608	2.9	0.58	3.0	.0690	0.5	47
3.1	0.13	273	161	0.61	19.7	519.8	3.8	605	56	.0601	2.6	0.70	2.7	.0840	0.8	16
2.2	0.00	312	101	0.33	22.7	524.2	3.9	590	45	.0596	2.1	0.70	2.2	.0847	0.8	12
6.2	0.19	313	146	0.48	22.8	524.9	3.5	560	54	.0588	2.5	0.69	2.6	.0848	0.7	7
7.2	0.00	287	137	0.49	21.0	526.4	3.6	577	41	.0593	1.9	0.70	2.0	.0851	0.7	10
10.2	0.18	244	69	0.29	17.9	527.7	3.9	398	59	.0546	2.6	0.64	2.7	.0853	0.8	-25
5.1	0.30	909	385	0.44	67.8	535.4	2.4	520	36	.0577	1.7	0.69	1.7	.0866	0.5	-3
8.2	-0.13	468	311	0.69	34.8	535.8	3.2	604	43	.0600	2.0	0.72	2.1	.0867	0.6	13
2.1	0.94	1103	661	0.62	93.6	601.7	3.1	701	58	.0628	2.7	0.85	2.8	.0978	0.5	17
4.1	0.36	274	91	0.34	26.1	675.0	6.5	521	106	.0578	4.8	0.88	4.9	.1104	1.0	-23
1.2	0.13	199	88	0.46	19.7	704.8	5.5	790	46	.0655	2.2	1.04	2.3	.1155	0.8	12
1.1	0.04	439	278	0.65	45.1	728.2	4.8	808	30	.0661	1.4	1.09	1.6	.1196	0.7	11
9.2	-0.15	174	69	0.41	30.3	1188.6	8.0	1216	42	.0808	2.2	2.25	2.3	.2025	0.7	2
A8-06 Nogoli Metamorphic Complex																
4.2	3.67	409	63	0.16	23.9	408.4	9.2	327	593	.0530	26.1	0.48	26.2	.0654	2.3	-20
12.2	2.06	451	15	0.03	26.5	418.8	3.1	652	148	.0614	6.9	0.57	6.9	.0671	0.8	56
6.3	0.25	161	59	0.38	10.9	488.9	5.6	492	105	.0570	4.8	0.62	4.9	.0788	1.2	1
1.2	0.43	145	41	0.30	10.1	500.5	6.6	601	116	.0599	5.3	0.67	5.5	.0807	1.4	20
3.2	0.68	358	58	0.17	25.4	508.4	4.9	288	165	.0521	7.2	0.59	7.3	.0821	1.0	-43
7.2	0.97	92	16	0.18	6.6	512.7	8.4	317	216	.0527	9.5	0.60	9.7	.0828	1.7	-38
2.2	0.27	310	53	0.18	22.4	519.5	3.6	573	61	.0592	2.8	0.68	2.9	.0839	0.7	10
6.2	0.30	312	31	0.10	22.9	526.7	4.0	492	55	.0570	2.5	0.67	2.6	.0851	0.8	-7
8.2	0.19	433	232	0.55	32.0	530.1	3.1	456	46	.0561	2.1	0.66	2.2	.0857	0.6	-14
6.1	8.48	1460	107	0.08	118.0	532.2	6.4	676	280	.0620	13.1	0.74	13.1	.0861	1.3	27
8.1	-0.31	72	73	1.05	5.4	541.7	7.3	715	94	.0632	4.4	0.76	4.7	.0877	1.4	32
5.2	-0.44	216	60	0.29	16.5	552.1	5.3	575	91	.0592	4.2	0.73	4.3	.0894	1.0	4
9.2	1.38	208	95	0.47	16.2	552.8	5.5	594	177	.0597	8.2	0.74	8.2	.0895	1.0	7
10.1	0.82	122	27	0.23	10.9	633.8	6.5	328	142	.0530	6.2	0.75	6.3	.1033	1.1	-48
11.2	0.20	654	43	0.07	58.7	639.2	3.5	596	36	.0598	1.7	0.86	1.8	.1042	0.6	-7
9.1	-0.35	357	170	0.49	32.6	654.2	4.6	804	50	.0659	2.4	0.97	2.5	.1068	0.7	23
A73-05 Conlara Metamorphic Complex																
1.2	0.21	785	24	0.03	56.8	518.5	30.5	581	52	.0594	2.4	0.69	6.6	.0838	6.1	12
8.2	0.19	433	45	0.11	34.3	566.8	3.8	690	51	.0625	2.4	0.79	2.5	.0919	0.7	22
5.2	0.35	245	97	0.41	20.8	604.4	35.5	721	64	.0634	3.0	0.86	6.8	.0983	6.1	19
16.1	0.70	152	14	0.10	13.3	621.6	6.9	837	134	.0670	6.4	0.93	6.5	.1012	1.2	35
20.1	0.74	57	11	0.21	5.2	643.3	9.0	501	179	.0572	8.1	0.83	8.2	.1049	1.5	-22
17.1	0.12	465	153	0.34	45.5	695.3	3.6	653	34	.0614	1.6	0.96	1.7	.1139	0.5	-6
15.1	0.41	159	31	0.20	16.2	720.1	6.1	633	99	.0608	4.6	0.99	4.7	.1182	0.9	-12
14.2	2.57	82	44	0.55	8.5	723.0	14.1	631	422	.0608	19.6	0.99	19.7	.1187	2.1	-13
14.1	0.32	177	136	0.80	19.2	767.0	6.7	707	69	.0630	3.2	1.10	3.4	.1263	0.9	-8
3.2	0.23	327	45	0.14	36.9	792.4	45.7	1075	36	.0752	1.8	1.36	6.4	.1308	6.1	36
1.1	0.11	664	69	0.11	77.2	814.8	46.8	751	24	.0643	1.1	1.20	6.2	.1347	6.1	-8
12.2	1.92	68	10	0.14	8.1	819.8	18.4	318	563	.0528	24.8	0.99	24.9	.1356	2.4	-61
8.1	2.23	37	9	0.26	5.1	940.8	68.5	544	288	.0584	13.2	1.26	15.3	.1571	7.8	-42
21.1	0.30	87	87	1.03	12.2	973.4	9.6	917	73	.0696	3.5	1.56	3.7	.1630	1.1	-6
13.1	0.15	366	101	0.28	52.3	991.1	5.7	1033	31	.0737	1.5	1.69	1.7	.1662	0.6	4
7.2	0.24	301	142	0.49	43.4	995.8	5.9	981	41	.0718	2.0	1.65	2.1	.1671	0.6	-2
5.1	0.12	207	31	0.15	30.7	1022.8	58.0	1059	41	.0746	2.0	1.78	6.4	.1719	6.1	4
10.2	0.04	399	170	0.44	60.7	1051.5	4.8	1034	21	.0737	1.1	1.80	1.2	.1772	0.5	-2
18.1	-0.14	105	69	0.67	16.1	1059.6	8.8	1032	43	.0737	2.1	1.81	2.3	.1786	0.9	-3
6.1	1.46	118	58	0.51	18.9	1079.6	61.2	1089	135	.0758	6.7	1.91	9.1	.1823	6.1	1
2.1	1.09	146	61	0.43	23.7	1101.3	62.2	1008	96	.0728	4.7	1.88	7.7	.1863	6.1	-8
3.1	0.42	198	117	0.61	32.6	1122.8	63.2	1068	51	.0750	2.5	1.97	6.6	.1903	6.1	-5
4.1	0.12	431	34	0.08	75.7	1192.9	66.6	1055	24	.0745	1.2	2.10	6.2	.2033	6.1	-12
9.2	0.76	316	268	0.88	57.3	1225.8	8.6	1056	55	.0745	2.7	2.15	2.8	.2094	0.8	-14
11.2	0.11	307	85	0.29	92.6	1936.9	10.9	1862	16	.1138	0.9	5.50	1.1	.3505	0.7	-4
19.1	0.04	336	256	0.79	137.8	2514.2	11.2	2681	7	.1831	0.4	12.04	0.7	.4770	0.5	7
A93-05 San Luis Formation																
6.1	2.64	301	247	0.85	12.6	297.8	18.2	1887	127	.1154	7.1	0.76	9.4	.0473	6.2	534
2.1	16.41	1673	1925	1.19	100.3	364.4	22.1	3049	55	.2296	3.4	1.85	7.1	.0582	6.2	737
1.1	20.81	1268	4945	4.03	93.8	423.6	25.4	2653	100	.1800	6.1	1.69	8.7	.0679	6.2	526
3.1	0.97	255	146	0.59	20.2	560.6	33.1	512	114	.0575	5.2	0.72	8.0	.0909	6.1	-9
4.1	0.51	210	98	0.48	17.2	582.7	34.3	786	127	.0654	6.1	0.86	8.6	.0946	6.1	35
5.1	0.66	500	813	1.68	41.4	587.2	34.4	501	69	.0572	3.1	0.76	6.9	.0954	6.1	-15
7.1	0.48	236	112	0.49	19.5	587.7	34.5	535	99	.0581	4.5	0.77	7.6	.0955	6.1	-9
9.1	0.13	336	212	0.65	25.8	549.3	32.3	655	51	.0614	2.4	0.76	6.6	.0889	6.1	19
11.1	0.35	247	153	0.64	19.3	557.8	32.8	614	94	.0603	4.3	0.75	7.5	.0904	6.1	10
8.1	0.45	337	217	0.67	26.5	561.2	33.0	518	60	.0577	2.8	0.73	6.7	.0910	6.1	-8
7.2	0.27	216	133	0.64	17.1	562.9	34.2	651	61	.0613	2.9	0.77	6.9	.0913	6.3	16
10.1	0.52	191	238	1.29	15.5	577.2	34.0	697	90	.0627	4.2	0.81	7.5	.0937	6.1	21
12.1	0.51	143	94	0.68	11.9	590.0	34.7	684	93	.0623	4.3	0.83	7.5	.0958	6.1	16

indicating moderate feldspar alteration and an average for the metapelitic rocks of 71 ($n = 10$), indicating a moderate degree of alteration in the source area. This value is similar to that of the average shales (CIA = 70–75; Nesbit and Young, 1982). In the A–CN–K diagram, only some of the samples plot close to the A–K line (Fig. 4), implying that weathering in the source area was simply the breakdown of plagioclase, corresponding to intermediate chemical weathering according to the scheme suggested by Fedo et al. (1995). Two samples from the PMC, three from SLF and two from PVF plot closer to the A–K line. The inferred composition of the source indicates an average granodioritic composition for the PVF and the CMC, whereas the PMC shows two different tonalitic and feldspar rich sources.

6. Provenance analysis

6.1. Major and trace elements implications

Most of the samples are pelites, greywackes, litharenites or arkoses (Fig. 5). The samples plot in areas comparable to the samples from Sims et al. (1998), Brogioni (2001), López de Luchi et al. (2003) and Zimmermann (2005), except for one metapsammitic rock from the SLF (A12-06) and two samples from the PMC (A13-06 and A19-06) that are shifted due to higher SiO_2/Al_2O_3 ratios. One metapelitic sample from the SLF yielded a high Al_2O_3 concentration (21%) and a low log (Fe_2O_3/K_2O).

The PMC and the SLF are characterised by a bimodal distribution with rocks below 65% SiO_2 or above 72%, the more recycled sources shown by the more silica-rich rocks. The SiO_2/Al_2O_3 ratios are bracketed between 3.45 and 5.8. The metapsammites exhibit high Zr/Sc values and all the samples of the PMC show higher Th/Sc quotients at given values of Zr/Sc than the rest of the analysed rocks suggesting more granitic or recycled sources. Samples that show lower Zr/Sc ratios exhibit Th/Sc values similar to the SLF (A9-06, A15-06, A85-06 and A86-06). The Cr/V quotient is almost constant, but Y/Ni tend to higher values indicating the influence of heavy minerals in the silica-rich samples. These features are partly shared by the NMC. The samples of the CMC and the PVF lack a bimodal distribution, and most of the analysed ratios like the Th/Sc or Y/Ni are similar in both units.

The Th/Sc vs. Zr/Sc diagram (Fig 10) points to moderate sediment recycling in general, with two exceptions from the PMC (A13-06 and A19-06). The CMC and the PVF show comparable Th/Sc ratios, but although Zr/Sc is relatively low, the CMC shows higher values than the PVF. Cr/V and Y/Ni ratios (Figs. 8 and 9) indicate no major mafic contribution, which is arguing against dominant volcanic input into the basin and the presence of ophiolites (Cr/V). Both the CMC and the PVF show constant and low Cr/V quotients and a limited increase in Y/Ni, which suggests a compositional uniform source and probably less recycling than the SLF or the PMC.

The Eu/Eu^* anomalies of around 0.60 in the PVF and the Sierra de San Luis are typical for the UCC (0.65). In contrast several samples from previous workers in the CMC show a less pronounced Eu/Eu^* anomaly between 0.8 and 0.9 (López de Luchi et al., 2003), indicating plagioclase enrichment in the sediments (Taylor and McLennan, 1985). The source area should be dominated by granodioritic to granitic material from a continental arc.

Tectonic diagrams using major (Fig. 6) and trace elements (Figs. 7–12) suggest an active margin with an acidic arc as the source rock for the sediments in the Sierra de San Luis and the PVF. López de Luchi et al. (2003) proposed a continental island-arc or an active continental margin for the Sierra de San Luis metaclastic rocks, which agrees with the results in this study. Although most of the data plot in the continental island-arc field, La/Sc ratios are higher than the normal values for the rocks of this tectonic setting (Fig. 12b).

López de Luchi et al. (2003) used the high Th/U values to exclude a fore-arc setting for the metaclastic rocks of San Luis. Zimmermann (2005) suggested that high Th/U may be derived from weathering, which would be accompanied by a positive Ce anomaly. Since no Ce anomaly is shown in our data collection, evidence of weathering is not very strong. The higher average ratios of Th/U from the PMC and the NMC may suggest a back-arc basin, whereas the SLF, the CMC and the PVF show more scattered values.

A group of samples from the PMC with lower La/Th, relatively higher La/Sc ratios and a trend to higher Hf contents may correspond to more felsic/recycled sources and a more defined trend towards a continental arc or even a passive margin in tectonic diagrams. The rest of the samples from the PMC also show higher La/Sc values at given Ti/Zr ratios, but no clear Hf enrichment and point to an active continental margin. The PMC could have been fed from different sources, i.e. a recycled or felsic source and an active margin which would imply a shorter transportation.

6.2. Implications for whole rock Sm–Nd data

The recalculation of the Sm–Nd model ages for the metaclastic units of the Eastern Sierras Pampeanas (Rapela et al., 1998; Bock et al., 2000; Steenken et al., 2004; Escayola et al., 2007 among others) using the one stage model of Goldstein et al. (1984) yielded T_{DM} ages between 1.8–1.5 Ga. The new T_{DM} ages between 1.8 and 1.6 Ga and $\varepsilon Nd_{(540\ Ma)}$ values between −6.3 and −3.9 are in accordance to previously published Nd data of Bock et al. (2000) for the PVF (T_{DM} ages between 1.8 and 1.6 Ga and $\varepsilon Nd_{(540\ Ma)}$ data between −6.4 and −5.7). The two metashales (A85-06 and A86-06) with the youngest T_{DM} ages and the highest $\varepsilon Nd_{(540\ Ma)}$ values also exhibit the lowest Th/Sc ratios (0.75 and 0.73). This could point to a juvenile input, lowering the T_{DM} ages and raising the $\varepsilon Nd_{(540\ Ma)}$. Excluding these two samples, the PVF and the Arequipa–Antofalla basement Nd model ages exhibit a nearly complete overlap, making the latter a possible source for these metasediments.

Metapsammites of the CMC are very homogeneous with T_{DM} ages between 1.69 and 1.65 Ga and $\varepsilon Nd_{(540\ Ma)}$ data between −5.3 and −4.8. Sample A61-05 which did not show any chemical indication of a volcanic or juvenile input gives the lowest T_{DM} age of 1.54 Ga and the highest $\varepsilon Nd_{(540\ Ma)}$ of −3.0. This data are in contrast to Steenken et al. (2004), who published two T_{DM} ages of 1.83 and 1.80 Ga and $\varepsilon Nd_{(540\ Ma)}$ of −6.8 and −6.3. On the basis of this data, the CMC does not seem to be that homogeneous, as it was previously assumed.

The PMC shows T_{DM} ages between 1.73 and 1.64 Ga and $\varepsilon Nd_{(540\ Ma)}$ ratios between −6.0 and −5.3. Only the sample A13-06 shows an older T_{DM} age (1.83 Ga) and a lower $\varepsilon Nd_{(540\ Ma)}$ of −6.7, which would be comparable with the SLF. The T_{DM} ages between 1.70 and 1.64 Ga and $\varepsilon Nd_{(540\ Ma)}$ between −5.6 and −5.3 for the NMC are indistinguishable from the calculated dominant values for the CMC and the PMC. These ages and the $\varepsilon Nd_{(540\ Ma)}$ data are, although slightly more juvenile, comparable to the 1.66 and 1.56 Ga and the $\varepsilon Nd_{(540\ Ma)}$ −5.6 and −4.0 from Steenken et al. (2004).

Low-grade metapelites of the Eastern Sierras Pampeanas have a more evolved and restricted source than the PVF and the other basement domains from the Sierra de San Luis. Four out of five $\varepsilon Nd_{(540\ Ma)}$ values from the SLF are between −7.8 and −6.6, whereas Steenken et al. (2004) reported $\varepsilon Nd_{(540\ Ma)}$ of −8.1 and −7.5. Such low $\varepsilon Nd_{(540\ Ma)}$ ratios are less radiogenic in the eastern Sierras Pampeanas and comparable with those for the Los Túneles phyllites, i.e. −6.8 (Rapela et al., 1998) and the phyllites from the

Olta Formation in the Sierras de Chepes, i.e. −6.8 and −6.7 (Pankhurst et al., 1998).

In spite of the direct contact between the Eastern Sierras Pampeanas and the Río de la Plata craton (Rapela et al., 2007), T_{DM} ages of 2.7–2.2 Ga (Cingolani et al., 2002; Hartmann et al., 2002; Pankhurst et al., 2003; Rapela et al., 2007) typical for the Río de la Plata craton were not found in the Eastern Sierras Pampeanas. This excludes the Río de la Plata craton as an exclusive source for the metaclastic units. Rapela et al. (2007) proposed that the Arequipa–Antofalla basement was part of a major continental mass that included the Western Sierras Pampeanas and the Amazonia craton. This large continent would have collided with the Río de la Plata and the Kalahari cartons, to produce the Pampean orogeny that is responsible for the main metamorphic overprint of the CMC and the PVF (Steenken et al., 2007; Rapela et al., 2007). Rapela et al. (2007) raised the thesis that the PVF is related to the South African Saldania Group. This unit has Sm–Nd model ages between 1.6 and 1.5 Ga (da Silva et al., 2000) only slightly younger than the available data for the Eastern Sierras Pampeanas. The T_{DM} ages in the Arequipa–Antofalla craton cluster around 1.9 and 1.5 Ga (Lucassen et al., 2000), with one exception of 1.3 Ga, making it a possible source rock, too.

6.3. Whole rock Pb–Pb evidence

The linear cigar-shaped array defined by the new whole rock Pb data ($^{206}Pb/^{204}Pb$ 18.35–20.03, $^{207}Pb/^{204}Pb$ 15.63–15.76 and $^{208}Pb/^{204}Pb$ 38.59–40.31) does not distinguish the different domains of the Sierra de San Luis and the PVF. The only difference can be seen in the evolution of the $^{208}Pb/^{204}Pb$ of the PMC that seems to evolve in a trend, flatter than those of the other domains, which would point to a different source, as already implied by the major and trace elements.

The $^{207}Pb/^{204}Pb$ data is comparable to granitic gneisses from the Sunsás orogenic belt in southwestern Brazil (Geraldes et al., 2001) and to the Arequipa–Antofalla basement (Loewy et al., 2003, 2004). These authors compared the Northern Domain of the Arequipa–Antofalla block with the Richtersveld Domain (Kalahari craton) and Central Domain with the Natal belt (Kalahari craton). Such a distinction is not feasible in our data collection. The samples plot in an overlapping area ($^{207}Pb/^{204}Pb$ diagram Fig. 15). In the $^{208}Pb/^{204}Pb$ diagram (Fig. 16), the data also plots in an overlapping area of the Central Domain of the Arequipa–Antofalla basement, the Western Brazilian Shield, the Southern Domain of the Arequipa–Antofalla basement and the Natal belt, with one exception of the highly radiogenic sample A10-06 from the CMC. The Northern Domain of the Arequipa–Antofalla basement shows a steeper slope than the data from the Eastern Sierras Pampeanas for the $^{207}Pb/^{204}Pb$ vs. $^{206}Pb/^{204}Pb$ isotopic ratios, and thus, can be excluded as a possible source area for the metasedimentary rocks of the Eastern Sierras Pampeanas. There is only one sample from the SLF and one from the PVF that plots in this area. The Central Domain of the Arequipa–Antofalla basement can be divided into a northern area (Belén) and a southern area (Choja). There are no differences between these two areas in the $^{207}Pb/^{204}Pb$ vs. $^{206}Pb/^{204}Pb$ plot. However, in the $^{208}Pb/^{204}Pb$ vs. $^{206}Pb/^{204}Pb$ plot, the Pb ratios of the northern Belén area plot above our Pb data, but the southern Choja (Loewy et al., 2004) data is similar to the new results. This makes a provenance from the northern area of the Central Arequipa–Antofalla basement unlikely for the Eastern Sierras Pampeanas. If a provenance from the Arequipa–Antofalla basement is assumed, the provenance area has to be in the Central Choja Domain or in the Southern Domain. Similar data led Schwartz and Gromet (2004) to conclude that the Kalahari craton was a possible source for the metasedimentary rocks of the Eastern Sierras Pampeanas in Córdoba.

6.4. Constrains from the detrital SHRIMP ages

Provenance analysis by Shrimp data on zircons is mainly based on the presence of Grenvillian peaks in combination with Brasilano ages. The PVF and the CMC exhibit comparable peaks or at least both metaclastic units record an important Grenvillian provenance. These peaks also appear in other domains of the Eastern Sierras Pampeanas, for example in the Sierras de Córdoba and in the Sierra de Ancasti (Schwartz and Gromet 2004; Steenken et al., 2006; Rapela et al., 2007). Based on the Sm–Nd systematic and SHRIMP dating Steenken et al. (2004, 2006) suggested that the CMC is the high-grade equivalent of the PVF. The NMC almost (one from 29 spots) completely lacks Grenvillian inheritance, whereas the PMC records a subordinate peak at around 1.0 and one spot at 2.7 Ga (Steenken et al., 2006). In the CMC 26 age determinations (Figs. 17c and 18b) from a banded schist cover the spectrum from Pampean (519 Ma) up to the Proterozoic–Archaean limit (2514 Ma). The youngest analyses at 519 and 567 Ma were gained from low Th/U (0.03 and 0.11) zircon rims, pointing to a metamorphic growth. Inherited zircon ages start at 604 Ma and cover the Brasiliano and Grenvillian orogenic cycles. The two oldest grains represent magmatic activity at 1940 Ma, i.e. younger than the 2.0–2.2 Transamazonian orogeny and 2514 Ma. More important is the lack of any concordant Pampean ages. A lot of ages that point to Brasiliano events are discordant, and thus, the $^{207}Pb/^{206}Pb$ age should be preferred. These ages also point to Brasiliano events of different ages. The youngest reliable $^{207}Pb/^{206}Pb$ age can be found at 581 ± 52 Ma and should reflect the maximum age of deposition. In spite of the big error, this is not in conflict with a metamorphic PbSL garnet age of 564 ± 21 Ma (Siegesmund et al., 2009). Similar U–Pb zircon patterns were obtained at the NW sector of the CMC (Steenken et al., 2006), in the northern part of the Sierras de Córdoba (Sims et al., 1998; Schwartz and Gromet, 2004; Escayola et al., 2007), in the Sierra de Ancasti (Rapela et al., 2007) and in the PVF (Adams et al., 2006, 2008).

The majority of the zircons were derived from late Mesoproterozoic and Neoproterozoic sources, as documented by age clusters at 962 ± 17 Ma and 631 ± 15 Ma. Rapela et al. (2007) sampled the regionally developed banded schists of the Ancasti Formation in the Sierra de Ancasti. Detrital zircons exhibit a generally bimodal age distribution, dominated by Mesoproterozoic (1100–960 Ma) and Neoproterozoic (680–570 Ma) components. A minor component represented by late Palaeoproterozoic concordant grains is also observed (1936 Ma). Concordant zircons in the 2.26–2.02 Ga interval of the Río de la Plata craton are absent. These data from the CMC are comparable with those of Schwartz and Gromet (2004) for the banded schist of northern Sierra Grande de Córdoba. Adams et al. (2006, 2008) presented LA ICP-MS U/Pb single zircon data for the PVF. These detrital zircons have maxima around 600 Ma, 900–1000 Ma, a subordinate maximum around 1900 Ma and few Neoarchaean grains.

Samples of the NMC are dominated by a mostly magmatic Pampean event since geologically meaningful ages ($n = 22$) define a maximum around 530 Ma (Fig. 18a), although the ages can even be Famatinian (489 Ma, only 1% of discordance), which agrees with the monazite data from Steenken et al. (2006). Only one zircon indicates the Grenvillian orogeny. Palaeoproterozoic ages are not observable. A tailing of the ages which do not belong to the Pampean orogeny, up to about 730 Ma could be related to the Brasiliano orogeny (e.g. Leite et al., 2000). The absence of 2200 Ma ages excludes a Río de la Plata provenance. As zircon ages decrease relatively constant down to 489 Ma, no clear distinction can be made between the Pampean and the Famatinian orogenies. The lack of Grenvillian ages suggests a source different from those of the PVF or the CMC. The existence of a barrier may have prevented the deposition of Grenvillian material. This barrier could have been

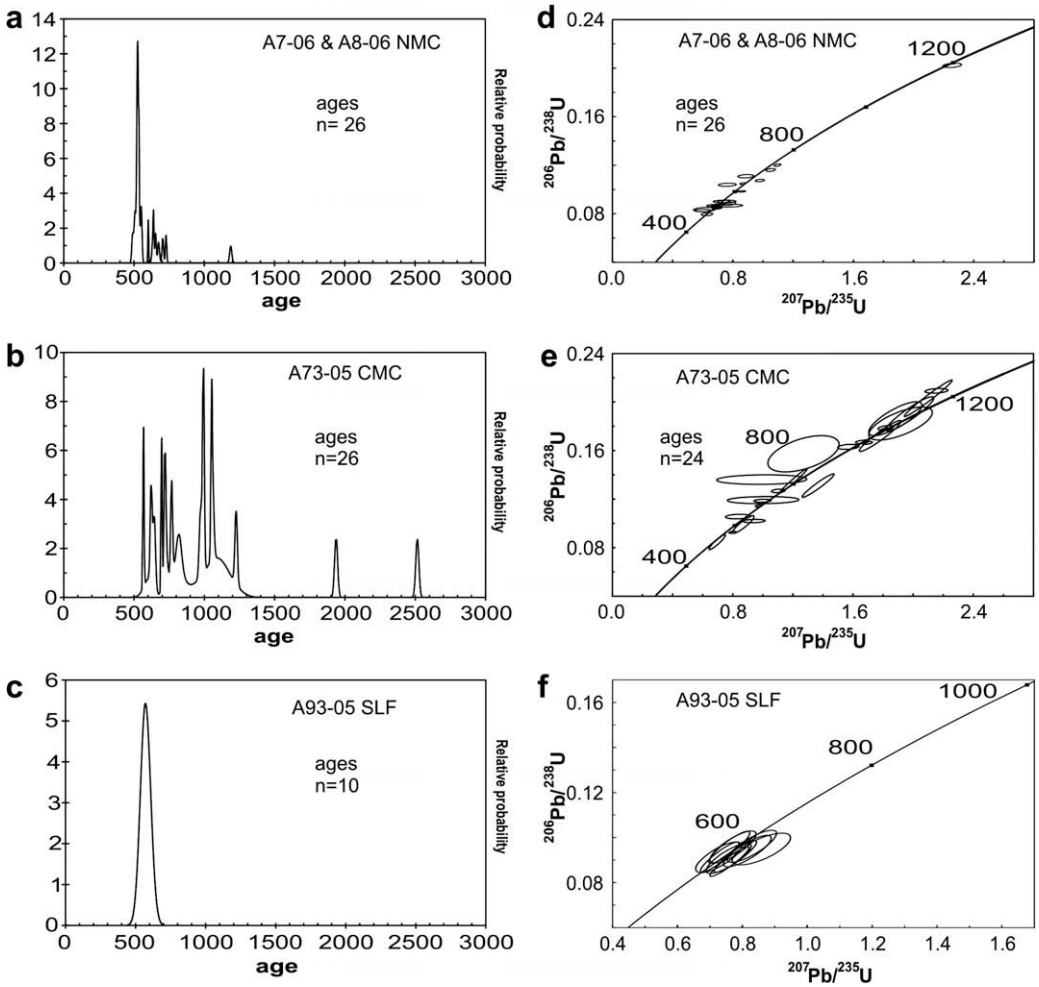

Fig. 18. Probability density plots of the $^{206}U/^{238}Pb$ SHRIMP ages (a–c). The Wetherill concordia diagrams for the samples are shown in d–f. The three most discordant samples are not shown in (f).

generated during the Pampean orogeny. The exhumation of rocks with a Pampean age signature may have resulted in a dilution of the Brasilano and Grenvillian input to the protolith of the NMC, the PVF and the SLF.

Detrital ages for the SLF (Fig. 18c) are bracketed between 590 Ma and 549 Ma (discordance between −15% and 35%). The striking difference to the rest of the complexes of the Sierra de San Luis is the narrow spread of zircon ages. Three zircon grains are extremely discordant and show Palaeoproterozoic and Archaean $^{207}Pb/^{206}Pb$ ages. Combining the data (by excluding the three discordant plots) results in a concordant (Fig. 18f) age of 569 ± 20 Ma (2σ, MSWD = 2.5), which is considered the age of the source area. On the basis of these ages, a more restricted source has to be assumed as the provenance for this sample which agrees with the Sm–Nd results. These do not necessarily require a more restricted, but at least a different source area than the other units.

Available SHRIMP zircon data for the PMC (Steenken et al., 2006) also show a marked Brasiliano–Pampean peak and one age of 1000 Ma (Fig 18d). This is similar to the new data from the NMC, making a comparable provenance likely. Llambías et al. (2003) reported early Pampean activity around 584 Ma generated by volcanic activity in the Sierra Norte de Córdoba. These ages are similar to the zircon ages of the SLF. Therefore, rocks of the Sierra Norte could be the source of the zircons in the SLF. The highly negative $\varepsilon Nd_{(540\ Ma)}$ data in the SLF shades doubt on a volcanic origin as volcanic activity should be connected to higher $\varepsilon Nd_{(540\ Ma)}$ values. Although only juvenile volcanic material elevates the εNd data, it remains unclear, why the SLF shows the lowest $\varepsilon Nd_{(540\ Ma)}$ values of all domains. The T_{DM} ages should also be younger than those in the other metamorphic complexes. Another possible source for the magmatically zoned zircons in the SLF are plutonic bodies. They can have a very restricted spread in zircon ages, and also show high T_{DM} ages and low εNd data (Las Verbenas tonalite, Steenken et al., 2004, 2006). This would make a plutonic complex very probable as the provenance for the SLF.

6.5. Tectonic model for the development of the western margin of Gondwana

Our new isotopic information, i.e. Sm–Nd, Pb isotopes and U/Pb SHRIMP data on zircons, together with previously published data (Sims et al., 1998; Rapela et al., 1998, 2007; Schwartz and Gromet, 2004; Steenken et al., 2004, 2006; Adams et al., 2008 among others) strongly argues against the Río de la Plata craton being a major source for the metasedimentary units in the Eastern Sierras Pampeanas and Cordillera Oriental although their present position is juxtaposed.

Detrital zircons of the PVF yielded a cluster of ages at 680–570 Ma and around 1000 Ma. Additional smaller groups between those principal populations cover the entire range of the Pan-African–Brazilian orogeny. Older ages only occur subordinately (cf. Adams et al., 2006, 2008). The age spectrum is similar

to those of the Sierras de Córdoba (e.g. Schwartz and Gromet, 2004) and also similar to the CMC (Steenken et al., 2006; this paper). Those Brazilian and Grenvillian ages cannot be derived from the Palaeoproterozoic Río de la Plata craton. They can be found in the orogens east of the Río de la Plata craton and around the Kalahari craton like the Damara orogenic belt, the East Antarctic orogen, the Namaqua–Natal belt and the Dom Feliciano–Gariep belt (Scheepers and Armstrong, 2002; Basei et al., 2005; Eglington, 2006). Those orogens were juxtaposed after the closure of the Adamastor Ocean by the collision of the Río de la Plata craton, the Congo craton and the Kalahari craton (e.g. Chemale et al., 1995; Frimmel et al., 1996; Rozendaal et al., 1999; Basei et al., 2005). Collision and subsequent uplift of these regions exposed the rocks to erosion and the derived sediments may be deposited in the Puncoviscana trough. Later on the Puncoviscana trough was laterally displaced (Fig. 19) against the Río de la Plata craton in a dextral movement (Rapela et al., 2007; Casquet et al., 2008). This model includes the uplift of Grenvillian age rocks along the "western" margin of the Amazonian craton (i.e. the Sunsás arc, e.g. Cordani et al., 2000) by the collision of Amazonia with Laurentia.

The basement of the Eastern Sierras Pampeanas basins, on which the Grenvillian and Brasiliano detritus was deposited should be of Kalahari origin (Rapela et al., 2007). This is questionable as the basement below the PVF and the CMC is not exposed.

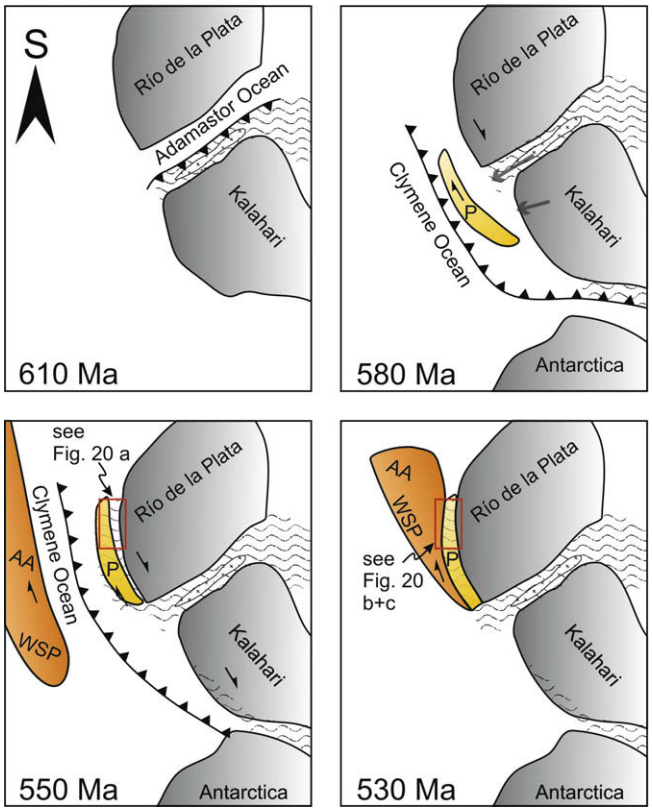

Fig. 19. Model of the formation of western Gondwana between 610 Ma and 530 Ma (modified after Rapela et al., 2007). The Río de la Plata craton approaches the Kalahari craton, which is associated with a subduction zone under the Kalahari craton and the formation of a magmatic arc. After the collision of the continents and uplift of the magmatic arc (580 Ma), the erosional material (grey arrows) was deposited onto the Pampean basement (P, Pampean Terrane). This basement was moved along dextral shear zones adjacent to the Río de la Plata craton. At 550 Ma, a big continental mass including parts of the Arequipa–Antofalla basement (AA) and the Western Sierras Pampeanas (WSP) converged and subduction below the Pampean basement started. The Arequipa–Antofalla basement and the Western Sierras Pampeanas collided with the Pampean Terrane at around 530 Ma.

The Clymene Ocean that started spreading around 774 Ma (Baldo et al., 2006) and later divided the proto West Gondwana from the Amazonia craton (Trindade et al., 2006) became inverted at around 550 Ma. This was due to the approach of a large continental mass (Amazonia, Arequipa–Antofalla and Western Sierras Pampeanas), which underwent right-lateral collision with the Rio de la Plata and Kalahari cratons, triggering the Pampean orogeny (see Fig. 20).

The correlation between the protoliths of the CMC and the PVF is largely based on the U/Pb zircon age inheritance patterns. Both units have a bimodal distribution of zircon ages with peaks at 630-580 Ma and around 1000 Ma (Steenken et al., 2006; Adams et al., 2006, 2008, this paper). A probable source for the sediments of the PVF might be the Dom Feliciano belt, e.g. the Florianópolis–Pelotas–Aiguá granite batholiths as it was already proposed by Rapela et al. (2007). Although this orogeny occurred around 600 Ma, available detrital magmatic zircons always occur accompanied by Grenvillian ages (Basei et al., 2000; Preciozzi et al., 2001; Adams et al., 2008).

Extensional tectonics after the deposition and deformation of the PVF and the CMC created the conditions for the development of the sedimentary basins in which the protoliths of the NMC, the PMC and the SLF were deposited. The LP/HT metamorphism and the (ultra)mafic bodies in the PMC (Hauzenberger et al., 2001) suggest a relatively thin crust, which argues for a back-arc basin as the tectonic setting for the protoliths of the metaclastic units of the PMC. Age constraints between 500 and 480 Ma were calculated for those (ultra) mafic rocks (Sims et al., 1998; Steenken et al., 2008), showing that extensional tectonic processes and sedimentation in the central area of the Sierra de San Luis post-date the Pampean orogeny of the Sierras de Córdoba and are related to the Famatinian cycle (Sims et al., 1998). The impact of the Grenvillian ages is almost negligible within the NMC, PMC and SLF. This denotes a different provenance compared to the CMC and PVF, even though the Nd and Pb isotope data are similar for all units. A probable explanation might be the formation of an orogenic barrier, i.e. the Pampean orogen that inhibited the essential input of Grenvillian material but is in accordance with the slightly younger inheritance pattern in the NMC, PMC and SLF (730–530 Ma, Sims et al., 1998; Steenken et al., 2006). Furthermore, this model implies that the Grenvillian material is strongly diluted and the Pampean ages became ubiquitous.

The difference in the metamorphic grade between the PMC and the SLF could be interpreted as resulting from the higher metamorphic grade in the central areas of the basin, i.e. around the mafic intrusions, and the bigger uplift of the PMC in the later stages of development of the Sierras Pampeanas. The later docking of the Precordillera Terrane led to the Famatinian orogeny and to a reheating or extended heating of the PMC and the NMC. Due to the collision, the PMC shows a concordant metamorphic zircon age of 497.5 Ma (Steenken et al., 2006) and some ages in the NMC show similar ages of 489 Ma (A8-06). The collision of the Precordillera/Cuyania Terrane is regionally considered to be around 460–470 Ma. Therefore, the older ages like the age of the granulite facies metamorphism in the PMC could be related to the approach of the terrane and the development of a back-arc basin, resulting in a HT deformation.

$^{206}Pb/^{238}U$ ages for the NMC extend up to 730 Ma, excluding early Pampean activity as an exclusive source for this complex. Apparent ages for the PMC only increase up to 604 Ma with one exception of 999 Ma and one at 2664 Ma. This restriction is even stronger in the SLF with ages ranging from 590–550 Ma. The provenance area of these metaclastic units may be the Dom Feliciano belt, where ages around or slightly below 600 Ma were found (Basei et al., 2000; Leite et al., 2000). The problem of the PMC and the SLF remains as only few ages above 600 Ma are found.

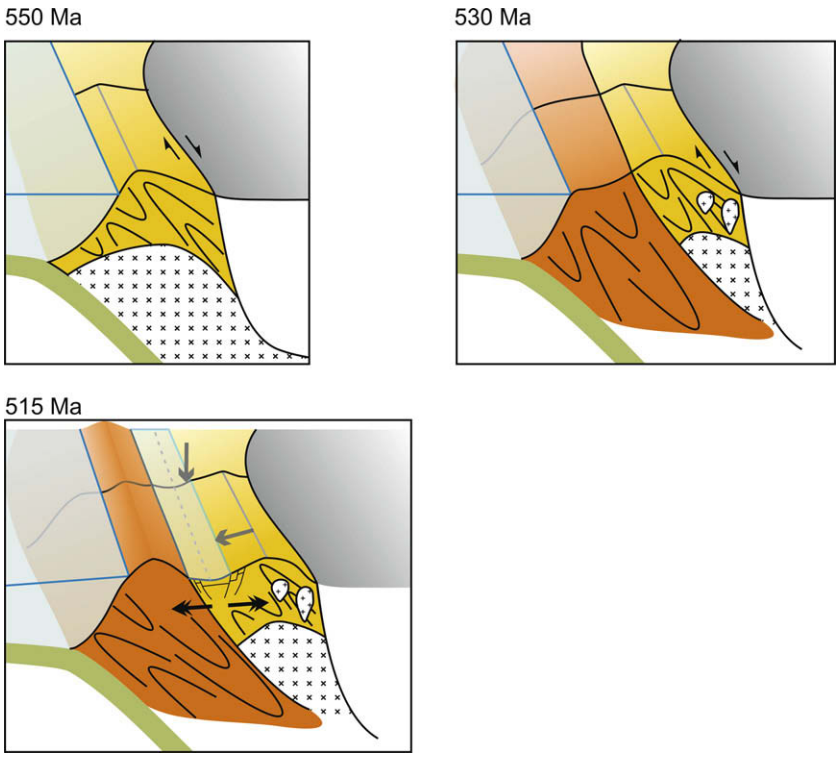

Fig. 20. At around 550 Ma the Pampean Terrane had been moved along dextral shear zones to its current position in relationship to the Río de la Plata craton (grey). Eastward directed subduction had just begun. The Puncoviscana Formation and its southern equivalents like the Conlara Metamorphic Complex (yellow) were already deformed. At 530 Ma, the Western Sierras Pampeanas (orange) collided with the Pampean Terrane. Around 535 Ma granitic bodies intruded the Puncoviscana Formation and equivalent units (Bachmann et al., 1987). Due to ongoing subduction a back-arc basin formed, in which the Nogolí Metamorphic Complex, the Pringles Metamorphic Complex and the San Luis Formation were deposited (grey arrows).

However, the Brasiliano orogens always have a broader data spread and could only be related to the NMC.

The SLF and the PMC may have been fed by early magmatic activities in the Pampean orogen. Either by large granitoid bodies that can be very limited in the spread of the zircon ages (Las Verbenas tonalite, Steenken et al., 2006) or by volcanic activity in the Sierra Norte that were dated by Llambías et al. (2003), yielding 584 Ma. The basin in which these sediments were deposited may have initially started as an intracratonic basin. Afterwards it turned into a back-arc basin when the Famatinian subduction started along the western margin of the Pampean orogen.

7. Conclusion

- A tectonic discrimination of the provenance areas based on *geochemical results*, between the different domains of the Sierra de San Luis and the PVF points to an active margin setting without being able to discriminate between fore-arc and back-arc setting. The PMC metapsammites are enriched in Th, pointing to a more felsic provenance. This unit shows the broadest dispersion of data with a mixed provenance of recycled, possibly passive margin material and relatively new felsic material. This can also be seen in the discriminataion diagrams from the *trace elements* for the tectonic setting. Most samples from the five investigated units plot in the field of an active continental margin or continental island-arc, except for some samples of the PMC that plot in the field of a passive margin. This bimodal tendency for the PMC can also be seen for the *major elements*. The difference in the tectonic setting using major elements is that some samples from the CMC and the PVF are shifted towards an oceanic arc, whereas the rest still plots in the active margin or continental island-arc field. This leads to the conclusion that the PMC is fed differently than the four other units. There are also differences between the NMC and the SLF on the one hand and the CMC and the PVF on the other hand.
- No clear distinction between the complexes of the Sierra de San Luis and the PVF is observed in the *Sm–Nd systematics*. T_{DM} ages and $\varepsilon Nd_{(540\ Ma)}$ data for all the units are bracketed between 1.5 and 1.8 Ga and −7.8 to −3.0. The SLF tends to show the less radiogenic $\varepsilon Nd_{(540\ Ma)}$ data and older T_{DM} ages than the other domains. The results from the PVF are very uniform, whereas the CMC shows younger T_{DM} ages and higher $\varepsilon Nd_{(540\ Ma)}$ values, which enlarges its compositional range, as compared with previously published results. Different sampling areas could explain this variation. The NMC has slightly younger and a more restricted range of T_{DM} ages and relatively higher $\varepsilon Nd_{(540\ Ma)}$ values. The PMC exhibits a big scatter in the data which is similar to the geochemistry.
- The *whole rock Pb isotopic data* of the different units plot in the same linear array. Using the Pb isotopes, discrimination seems to be difficult except for the $^{208}Pb/^{204}Pb$ vs. $^{206}Pb/^{204}Pb$ data from the PMC, in which a slightly different trend can be seen. The data plots in an area between (a) the Northern Domain of the Arequipa–Antofalla basement, which is similar to the Richtersveld domain in southern Africa and (b) the Central domain of the Arequipa–Antofalla basement which is congruent to the Natal belt in Namibia. The $^{207}Pb/^{204}Pb$ vs. $^{206}Pb/^{204}Pb$ data from the Northern domain of the Arequipa–Antofalla basement has a steeper slope than our data and can be excluded as a possible source. The northern part of the Central domain (Belén) can also be excluded as the source area, since the $^{208}Pb/^{204}Pb$ vs. $^{206}Pb/^{204}Pb$ plots above our data. Another clear result from the $^{207}Pb/^{204}Pb$ vs. $^{206}Pb/^{204}Pb$ plots is that the provenance of the different domains points to Gondwana and not Laurentia as

the source area. Whether the metasedimentary rocks have their origin in the Brazilian Shield, the Central- or Southern part or the Arequipa–Antofalla basement or if they are derived from southern Africa is not clearly indicated, as these areas have similar present day Pb isotopic data.
– The *U/Pb SHRIMP* technique gives the best insight into the provenance of the different investigated units. The absence of a Grenvillian peak in the NMC, the PMC and the SLF is the main difference to the CMC and the PVF. The NMC and the PMC seem to be built up by some material derived from the Pampean orogen and/or the Dom Feliciano–Gariep orogen. The units of the Sierra de San Luis became overprinted during the Famatinian orogenic cycle. The provenance of the SLF seems to be restricted to a certain Pampean dominated area. This could be an early volcanic or plutonic activity of the developing Pampean orogen, as only zircons around 570 Ma were found.

Acknowledgements

We are grateful for the German Science Foundation (DFG) Grant Si 438/28-1;2 that funded the research project. M.D. is grateful for the financial support from the DAAD for a 6-month short fellowship for Ph.D. students in Argentina. The manuscript was significantly improved by two anonymous reviewers.

Appendix A

A.1. Analytical techniques

For geochemical and isotope geochemical whole rock analyses, the sample material was broken following standard techniques using a jaw crusher and an agate mill. Major elements were analysed at the Geoforschungszentrum (GFZ) in Potsdam using a Panalytical XRF-PW 2400.

A.2. Whole rock geochemistry

Dissolution of the sample material for trace element measurements was performed in two parallel sessions at the Department of Geochemistry and Isotope Geology at the Geoscience Centre of the Georg-August-Universität in Göttingen (GZG). In the former department, the samples were digested in autoclaves as described in Heinrich and Herrmann (1990). Approximately 100 mg of sample powder was dissolved in 1 ml HF (40%) and 2 ml HNO_3 (65%) at 180 °C for at least 12 h. After drying, 1 ml HF (40%) and 1 ml $HClO_4$ (70%) were added and the samples were reheated up to 180 °C for another 12 h. Finally, the disintegrated sample was solved in 2 ml HNO_3 (65%) and diluted with H_2O up to 100 ml. In the Department of Isotope Geology, the time-pressure-dissolution gadget (Picotrace™) was used. Two milliliters HF (40%) and 1 ml HNO_3 (65%) were added to about 100 mg of sample powder and released after a reaction time of 3 h. Afterwards, the sample was dissolved in 2 ml HF (40%), 1 ml HNO_3 (65%) and 1 ml $HClO_4$ (70%) at 130 °C for at least 72 h. Subsequently, the acids were released at 140 °C, and 5 ml 6N HCl was added at 160 °C for at least 48 h. After releasing the HCl, nitrates were gained from the reaction product by adding 200 µl HNO_3 (65%). Finally the samples were dissolved in 2 ml HNO_3 (65%) and diluted up to 100 ml with H_2O. The same internal standard of known composition was used in both departments. A difference in the analyses between the two slightly different techniques in the two departments could not be observed. This was checked by comparing the data of some samples that were dissoluted in both ways.

ICP-MS measurements at the Department of Geochemistry were carried out using a Plasma Quad II+ from VG™. Analytical accuracy and precision were monitored using the standards JA-2, QC-1 and MA-N. The error is about 10–15% (2σ).

A.3. Nd-isotope data

Nd and Sm isotopic analyses were performed on representative samples by conventional isotope dilution technique. The samples were weighed into Teflon vials and spiked with a suitable amount of ^{150}Nd–^{149}Sm spike solution prior to dissolution in a mixture of 2 ml HF and 1 ml HNO_3 with a PicoTrace™ digestion system. The solutions were processed by standard cation-exchange techniques for purification of the Sm and Nd fractions. For the determination of isotopic compositions, Sm and Nd were loaded with 2.5 N HCl on pre-conditioned double Re filaments. Measurements of isotopic ratios were performed on a thermal ionisation mass spectrometer (TIMS) Finnigan Triton measuring in static mode (GZG, Department of Isotope Geology). Repeated measurement of the Nd inhouse standard yielded a $^{143}Nd/^{144}Nd$ ratio of 0.511798 ± 0.000077 ($n = 71$, 2σ) over the course of this study. The obtained Nd isotopic ratios of the samples were normalised to a $^{146}Nd/^{144}Nd$ ratio of 0.7219. Total procedure blanks were consistently below 150 pg for Sm and Nd. All $^{143}Nd/^{144}Nd$ ratios are reported with their 2σ internal precision plus the uncertainties resulting from the spike correction. The data were calculated according to the model of Goldstein et al. (1984).

A.4. Pb isotopic data

Rock powders were pretreated with HBr, dissolved with HF and HNO_3 during addition of HBO_3 (Connelly et al., 2006), and then dried and redissolved in HNO_3. Pb isotope ratios of whole rocks were analyzed at the Institute of Geography and Geology, University of Copenhagen, using a VG Sector 54 IT mass spectrometer. Chemical separation of Pb was performed over conventional anion exchange columns with HBr–HCl, followed by purification on 200-ml Teflon columns. Fractionation of Pb during static multi- collection-mode mass-spectrometric analysis was monitored by repeated analysis of the NBS 981 standard (Todt et al., 1993) and amounted to $0.105 \pm 0.008\%$ per atomic mass unit (amu; $n = 12$, 2σ). Procedural Pb blanks remained below 50 pg; this low blank does not affect the measured Pb-isotopic ratios of the samples significantly.

A.5. SHRIMP U/Pb zircon dating

Zircon grains were-hand selected and mounted in epoxy resin together with chips of the TEMORA (Middledale Gabbroic Diorite, New South Wales, Australia) and 91,500 (Geostandard zircon) reference zircons. The grains were sectioned approximately in half and polished. Reflected and transmitted light photomicrographs and cathodoluminescence (CL) SEM images were prepared for all zircons. The CL images were used to decipher the internal structures of the sectioned grains and to target specific areas within these zircons.

The U–Pb analyses of the zircons were made using the SHRIMP-II ionmicroprobe at the Centre of Isotopic Research, VSEGEI, St. Petersburg, Russia. Each analysis consists of five scans through the mass range. The diameter of the spot was about 25 µm and the primary beam intensity was about 2 nA. The data have been reduced in a manner similar to that described by Williams (1998, and references therein), using the SQUID Excel Macro of Ludwig (2000). The Pb/U ratios has been normalised relative to a value of 0.0668 for the $^{206}Pb/^{238}U$ ratio of the TEMORA reference zircons, equivalent to an age of 416.75 Ma (Black and Kamo, 2003). Uncertainties given for individual analyses (ratios and ages) are at the 1σ level;

however, the uncertainties in calculated concordia ages are reported at the 2σ level.

Appendix A. Supplementary data

Supplementary data associated with this article can be found in the online version, at doi:10.1016/j.jsames.2009.06.005.

References

Aceñolaza, F.G., Toselli, A.J., 1981.Geología del Noroeste Argentino. Publicación Especial de la Facultad de Ciencias Naturales, Uniersidad Nacional de Tucumán, 1287, 1–212.

Aceñolaza, F.G., Durand, F.R., 1986. Upper Precambrian–Lower Cambrian biota from the northwest of Argentina. Geological Magazine 123, 367–375.

Aceñolaza, G.F., Tortello, M.F., 2003. El Alisal: a new locality with trace fossils of the Puncoviscana Formation (late Precambrian–early Cambrian) in Salta province, Argentina. Geologica Acta 1, 95–102.

Aceñolaza, F.G., Miller, H., Toselli, A.J. (Eds.), 1983. La geología de la Sierra de Ancasti. Münstersche Forschungen zur Geologie und Paläontologie 59, 1–372.

Aceñolaza, F.G., Miller, H., Toselli, A.J., 1988. The Puncoviscan Formation (late Precambrian–early Cambrian). Sedimentology, tectonometamorphic history and age of the oldest rocks of NW Argentina. In: Bahlburg, H., Breitkreuz, C., Giese, P. (Eds.), The Southern Central Andes: Contribution to Structure and Evolution of an Active Continental Margin. Lecture Notes on Earth Sciences, vol. 17, pp. 25–38.

Aceñolaza, F.G., Miller, H., Toselli, A.J. (Eds.), 1990. El Ciclo Pampeano en el Noroeste Argentino. Universidad Nacional de Tucumán, Serie Correlación Geológica, vol. 4, pp. 1–227.

Aceñolaza, F.G., Miller, H., Toselli, A.J., 2000. The Pampean and Famatinian cycles – superimposed orogenic events in West Gondwana. In: Miller, H., Herve, F. (Eds.), Geoscientific Cooperation with Latin America. Zeitschrift für Angewandte Geologie Sonderheft, vol. 1, pp. 337–344.

Aceñolaza, F.G., Miller, H., Toselli, A.J., 2002. Proterozoic–early Paleozoic evolution in western South America – a discussion. Tectonopysics 354, 121–137.

Aceñolaza, F., Aceñolaza, G.F., 2005. La Formación Puncoviscana y unidades estratigráficas vinculadas en el Neoproterozoico – Cámbrico Temprano del Noroeste Argentino. Latin American Journal of Sedimentology and Basin Analysis 12 (2), 67–91.

Adams, C., Miller, H., Toselli, A.J., 2006. Maximum age and Provenance area of the Puncoviscana Formation Sediments (NW Argentina) based on detrital zircon geochronology – a pilot study. In: 11th Congreso Geológico Chileno Actas, vol. 1, Análisis de Cuenca, pp. 11–14.

Adams, C., Miller, H., Toselli, A.J., Griffin, W.L., 2008. The Puncoviscana Formation of northwest Argentina: U–Pb geochronology of detrital zircons and Rb–Sr metamorphic ages and their bearing on its stratigraphic age, sediment provenance and tectonic setting. Neues Jahrbuch für Geologie und Paläontologie – Abhandlungen 247 (3), 341–352.

Aitcheson, S., Harmon, R.S., Moorbath, S., Schneider, A., Soler, P., Soria-Escalante, E., Steele, G., Swainbank, I., Wörner, G., 1995. Pb isotopes define basement domains of the altiplano, central Andes. Geology 23, 555–558.

Astini, R.A., Benedetto, J.L., Vaccari, N.E., 1995. The early Paleozoic evolution of the Argentine Precordillera as a Laurentian rifted, drifted and collided terrane: a geodynamic model. Geological Society of America Bulletin 107, 253–273.

Bachmann, G., Grauert, B., Kramm, U., Lork, A., Miller, H., 1987. El magmatismo Cámbrico medio Cámbrico superior en el basamento del noroeste Argentino: Investigaciones isotópicas y geocronológicas sobre los granitoides de los complejos intrusivos Santa Rosa de Tastil y Cañani. In: 10th Congreso Geológico Argentino, vol. 4, pp. 125–127.

Bahlburg, H., 1990. The Ordovician basin in the Puna of NW Argentina and N Chile: geodynamic evolution from back-arc to foreland basin. Geotektonische Forschungen 75, 1–107.

Baldo, E., Casquet, C., Pankhurst, R.J., Galindo, C., Rapela, C.W., Fanning, C.M., Dahlquist, J., Murra, J., 2006. Neoproterozoic A-type magmatism in the Western Sierras Pampeanas (Argentina): Evidence for Rodinia break-up along a proto-Iapetus rift? Terra Nova 18, 388–394.

Basei, M.A.S., Siga Jr., O., Masquelin, H., Harara, O.M., Reis Neto, J.M., Preciozzi, F., 2000. The Dom Feliciano belt of Brazil and Uruguay and its foreland domain the Río de la Plata Craton. In: Cordani, U.G., Milani, E.J., Thomaz Filho, A., Campos, D.A. (Eds.), Tectonic Evolution of South America, pp. 311–334.

Basei, M.A.S., Frimmel, H.E., Nutman, A.P., Preciozzi, F., Jacob, J., 2005. A connection between the Neoproterozoic Dom Feliciano (Brazil/Uruguay) and Gariep (Namibia/South Africa) orogenic belts – evidence from a reconnaissance provenance study. Precambrian Research 139, 195–221.

Bhatia, M.R., 1983. Plate tectonics and geochemical composition of sandstones. The Journal of Geology 91, 611–627.

Bhatia, M.R., Crook, K.A., 1986. Trace elements characteristics of greywackes and tectonic setting discrimination of sedimentary basins. Contributions to Mineralogy and Petrology 92, 181–193.

Black, L.P., Kamo, S.L., 2003. TEMORA: a new zircon standard for U–Pb geochronology. Chemical Geology 200, 155–170.

Boles, J.R., Franks, S.G., 1979. Clay diagenesis in Wilcox Sandstones of Southwest Texas: implications of smectite digenesis on sandstone cementation. Journal of Sedimentary Petrology 49, 55–70.

Brito Neves, B.B., Campos Neto, M.C., Fuck, R.A., 1999. From Rodinia to Western Gondwana: an approach to the Brasiliano–Pan-African cycle and orogenic collage. Episodes 22 (3), 155–166.

Brogioni, M., 2001. Geología de los cuerpos Vioroco y El Fierro, faja máfica-ultramáfica del borde oriental de la Sierra de San Luis. Revista de la Asociación Geológica Argentina 56 (3), 281–292.

Bock, B., Bahlburg, H., Worner, G., Zimmermann, U., 2000. Tracing crustal evolution in the southern central Andes from late Precambrian to Permian with geochemical and Nd and Pb isotope data. The Journal of Geology 108, 515–535.

Casquet, C., Pankhurst, R.J., Galindo, C., Rapela, C.W., Fanning, C.M., Baldo, E., Dahlquist, J., González-Casado, J.M., Colombo, F., 2008. A deformed alkaline igneous rock–carbonatite complex from the Western Sierras Pampeanas, Argentina: Evidence for late Neoproterozoic opening of the Clymene Ocean? Precambrian Research 165 (3–4), 205–220.

Cerredo, M.E., López de Luchi, M.G., 2002. Application of provenance and tectonic setting diagrams on metamorphic rocks: the case of metamorphic units from Sierra de San Luis. In: Sixth Congreso de Mineralogía y Metalogenia, Facultad de Ciencias Exactas y Naturales, Universidad de Buenos Aires, pp. 77–83.

Chemale Jr., F., Hartmann, L.A., da Silva, L.C., 1995. Stratigraphy and tectonism of the Precambrian to early Paleozoic units of Southern Brazil and Uruguay – excursion guidebook. Acta Geológica Leopoldensia 42, 4–115.

Cingolani, C.A., Hartmann, L.A., Santos, J.O.S., McNaughton, N.J., 2002. U–Pb SHRIMP dating of zircons from the Buenos Aires Complex of the Tandilia Belt, Río de la Plata Craton, Argentina. In: 15th Congreso Geológico Argentino, Actas, vol. 1, pp. 149–154.

Connelly, J., Thrane, K., Krawiec, A., Garde, A., 2006. Linking the Palaeoproterozoic Nagssugtoqidian and Rinkian orogens through the Disko Bugt region ofWest Greenland. Journal of the Geological Society of London 163, 319–335.

Cordani, U.G., Sato, K., Teixeira, W., Tassinari, C.C.G., Basei, M.A.S., 2000. Crustal evolution of the South American platform. In: Cordani, U.G., Milani, E.J., Thomaz-Filho, A., Campos, D.A. (Eds.), Tectonic Evolution of South America. In: 31st International Geological Congress, Río de Janeiro, pp. 19–40.

Da Silva, L.C., Gresse, P.G., Scheepers, R., McNaughton, N.J., Hartmann, L.A., Fletcher, I., 2000. U–Pb SHRIMP and Sm–Nd age constraints on the timing and sources of the Pan-African Cape Granite Suite, South Africa. Journal of African Earth Sciences 30 (4), 795–815.

Delpino, S., Dimieri, L., Bjerg, E., Kostadinoff, J., Mogessie, A., Hoinkes, G., Hauzenberger, C., Felfernig, A., 2001. Geometric analysis and timing of structures on mafic–ultramafic bodies and high-grade metamorphic rocks in the Sierras de San Luis province, Argentina. Journal of South American Earth Sciences 14 (1), 101–112.

Delpino, S.H., Bjerg, E.A., Ferracutti, G.R., Mogessie, A., 2007. Counterclockwise tectonometamorphic evolution of the Pringles Metamorphic Complex, Sierras Pampeanas of San Luis (Argentina). Journal of South American Earth Sciences 23, 147–175.

DePaolo, D.J., Wasserburg, G.J., 1976. Nd isotopic variations and petrogenetic models. Geophysical Research Letters 3, 249–252.

Dickinson, W.R., Suczek, C.A., 1979. Plate tectonics and sandstone compositions. American Association of Petroleum Geology 63, 2164–2182.

Dinelli, E., Lucchini, F., Mordenti, A., Paganelli, L., 1999. Geochemistry of Oligocene-Miocene sandstones of the northern Apennines (Italy) and evolution of chemical features in relation to provenance changes. Sedimentary Geology 127, 193–207.

Do Campo, M., Ribeiro Guevara, S., 2002. Geoquímica de las secuencias clásticas de la Formación Puncoviscana (Neoproterozoico, NO Argentina), proveniencia y marco tectónico. In: 15th Congreso Geológico Argentino, Actas CD-ROM, Trabajo, p. 370.

Durand, F.R., 1996. La transición Precámbrico-Cámbrico en el sur de Sudamérica. In: Baldis, B., Aceñolaza, F.G. (Eds.), Early Paleozoic evolution in Northwest Gondwana. Universidad Nacionál de Tucumán, Serie Correlación Geológica, vol. 12, pp. 195–206.

Eglington, B.M., 2006. Evolution of the Namaqua–Natal belt, southern Africa – a geochronological and isotope geochemical review. Journal of African Earth Sciences 46, 93–111.

Escayola, M., Ramé, G., Kraemer, P.E., 1996. Caracterización y significado tectónico de las fajas ultramáficas de las Sierras Pampeans de Córdoba. In: 13th Congreso Geológico Argentino, Actas, vol. 3, pp. 421–438.

Escayola, M.P., Pimentel, M.M., Armstrong, R., 2007. Neoproterozoic backarc basin: sensitive high-resolution ion microprobe U–Pb and Sm–Nd isotopic evidence from the Eastern Pampean Ranges, Argentina. Geological Society of America 35 (6), 495–498.

Fedo, C.M., Nesbitt, H.W., Young, G.M., 1995. Unravelling the effects of potassium metasomatism in sedimentary rocks and paleosols, with implications for paleoweathering conditions and provenance. Geology 23, 921–924.

Finney, S.C., Gleason, J.D., Gehrels, G.G., Peralta, S.H., Aceñolaza, G., 2003. Early Gondwanan connection for the Argentine Precordillera Terrane. Earth and Planetary Sciences Letters 205, 349–359.

Floyd, P.A., Leveridge, B.E., 1987. Tectonic environment of the Devonian Gramscatho basin, south Cornwall; framework mode and geochemical evidence from turbidite sandstones. Journal of the Geological Society 144, 531–532.

Frimmel, H.E., Hartnady, C.J.H., Koller, F., 1996. Geochemistry and tectonic setting of magmatic units in the Pan-African Gariep belt, Namibia. Chemical Geology 130, 101–121.

Geraldes, M.C., von Schmus, W.R., Condie, K.C., Bell, S., Teixeira, W., Babinski, M., 2001. Proterozoic geologic evolution of the SW part of Amazonian craton in Mato Grosso state, Brazil. Precambrian Research 111, 91–128.

Goldstein, S.L., O'Nions, R.K., Hamilton, P.J., 1984. A Sm–Nd isotopic study of atmospheric dusts and particulates from major river systems. Earth and Planetary Science Letters 70, 221–236.

González, P.D., Sato, A.M., Basei, M.A., Vlach, S, Llambías, E., 2002. Structure, metamorphism and age of the Pampean–Famatinian orogenies in the western Sierra de San Luis. In: Cabaleri, N., Linares, E., López de Luchi, M.G., Ostera, H. Panarello, H. (Eds.), 15th Congreso Geológico Argentino, Actas, vol. 11, pp. 51–56.

Grandstaff, D.E., Edelman, M.J., Foster, R.W., Zbinden, E., Kimberly, M.M., 1986. Chemistry and mineralogy of Precambrian paleosols at the base of the Dominion and Pongola Groups, Transvaal, South Africa. Precambrian Research 32, 97–131.

Harnois, L., 1988. The CIW index: a new chemical index of weathering. Sedimentary Geology 55, 319–322.

Hartmann, L.A., Santos, J.O.S., Cingolani, C.A., McNaughton, N.J., 2002. Two Palaeoproterozoic orogenies in the evolution of the Tandilia belt, Buenos Aires, as evidenced by zircon U–Pb SHRIMP geochronology. International Geology Review 44, 528–543.

Hauzenberger, C., Mogessie, A., Hoinkes, G., Felfernig, A., Bjerg, E., Kostadinoff, J., Delpino, S., Dimieri, L., 2001. Metamorphic evolution of the Sierras de San Luis, Argentina: Granulite facies metamorphism related to mafic intrusions. Mineralogy and Petrology 71 (1–2), 95–126.

Heinrich, H., Herrmann, A.G., 1990. Praktikum der Analytischen Geochemie. Springer, Berlin. p. 669.

Herron, M.M., 1988. Geochemical classification of terrigenous sands and shales from core or log data. Journal of Sedimentary Petrology 58, 820–829.

Hiscott, R.N., 1984. Ophiolitic source rocks for Taconic-age flysch: trace-element evidence. Geological Society of America Bulletin 95, 1261–1267.

Iacumín, M., Piccirillo, E.M., Girardi, V.A.V., Teixeira, W., Bellieni, G., Etcheveste, H., Fernández, R., Pinese, J.P.P., Ribot, A., 2001. Early Proterozoic calc-alkaline and Middle Proterozoic tholeiitic dyke swarms from central-eastern Argentina: petrology, geochemistry, Sr–Nd isotopes and tectonic implications. Journal of Petrology 42, 2109–2143.

Jahn, B.M., Condie, K.C., 1995. Evolution of the Kaapvaal Craton as viewed from geochemical and Sm–Nd isotopic analyses of cratonic pelites. Geochimica et Cosmochimica Acta 59, 2239–2258.

Janasi, V.A., Leite, R.J., van Schmus, W.R., 2001. U–Pb chronostratigraphy of the granitic magmatism in the Agudos Grandes Batholith (west of Sao Paulo, Brazil) – implications for the evolution of the Ribeira belt. Journal of South American Earth Sciences 14, 363–376.

Ježek, P., Miller, H., 1986. Deposition and fades distribution of turbiditic sediments of the Puncoviscana Formation (Upper Precambrian–Lower Cambrian) within the basement of the NW Argentine Andes. Zentralblatt für Geologie und Paläontologie 1 (9–10), 1235–1244.

Kay, S., Orrell, S., Abbruzzi, J.M., 1996. Zircon and whole rock Nd–Pb isotopic evidence for a Grenville Age and a Laurentian origin for the basement of the Precordillera in Argentina. The Journal of Geology 104, 637–648.

Keppie, J.D., Bahlburg, H., 1999. Puncoviscana Formation northwestern and central Argentina: passive margin or foreland basin deposit? Geological Society of America Special Paper 336, 139–143.

Kilmurray, J.O., Dalla Salda, L., 1977. Caracteres estructurales y petrológicos de la region central y sur de la Sierra de San Luis. Obra del Centenario del Museo de La Plata 4, l67–178.

Kraemer, P.E., Escayola, M.P., Martino, R.D., 1995. Hipótesis sobre la evolución neoproterozoica de las Sierras Pampeanas de Córdoba (30 84′–32 84′S) Argentina. Revista de la Asociación Geológica Argentina 50 (1–4), 47–59.

Llambías, E.J., Sato A.M, Ortiz Suárez, A., Prozzi, C. 1998. The granitoids of the Sierra de San Luis. In: Pankhurst, R.J., Rapela, C.W. (Eds.), The Proto-Andean Margin of Gondwana. Geolological Society of London, Special Publication, vol. 142, pp. 325–341.

Llambías, E.J., Gregori, D., Basei, M.A.S., Varela, R., Prozzi, C., 2003. Ignimbritas riolíticas neoproterozoicas en la Sierra Norte de Córdoba: ¢evidencia de un arco magmático temprano en el ciclo Pampeano? Revista de la Asociación Geológica Argentina 58 (4), 572–582.

Leite, J.A.D., Hartmann, L.A., Fernandes, L.A.D., McNaughton, N.J., Soliani Jr., E., Koester, E., Santos, J.O.S., Vasconcellos, J.O.S., Vasconcellos, M.A.Z., 2000. Zircon U–Pb SHRIMP dating of the Dom Feliciano belt, southernmost Brazil. Journal of South American Earth Sciences 13, 739–750.

Loewy, S., Connelly, J.N., Dalziel, I.W.D., Gower, C.F., 2003, Eastern Laurentia in Rodinia: constraints from whole-rock Pb and U–Pb geochronology. In: Sircombe, K.N., McElhinny, M.W. (Eds.), Orogenic Belts, Regional and Global Tectonics: A Memorial Volume to Chris McAulay Powell. Tectonophysics, vol. 375, pp. 169–197.

Loewy, S.L., Connelly, J.N., Dalziel, I.W.D., 2004. An orphaned basement block: the Arequipa–Antofalla basement of the central Andean margin of South America. Geological Society of America Bulletin 116, 171–187.

López de Luchi, M.G., 1986. Geología y Petrología del basamento de la Sierra de San Luis, Región del Batolito de Renca. Ph.D. Thesis, Departamento de Geología, Facultad de Ciencias Exactas, Universidad de Buenos Aires, pp. 1–374

López de Luchi, M.G., 1987. Caracterización geológica y geoquímica del Plutón La Tapera y del Batolito de Renca, Sierra de San Luis. In: 10th Congreso Geológico Argentino, Actas, vol. 4, pp. 84–87.

López de Luchi, M.G., 1996. Enclaves en un batolito postectónico: petrología de los enclaves microgranulares del batolito de Renca. Revista de la Asociación Geológica Argentina 51 (2), 131–146.

López de Luchi, M.G., Cerredo, M.E., Rossello, E., 1999. Protoliths of a metasedimentary sequence: a case study on the Lower Paleozoic Pacific margin of Gondwana. Annual Meeting of the Geological Society of America. Abstracts with Programs 31 (7), A298, Denver.

López de Luchi, M.G., Cerredo, M.E., Siegesmund, S., Steenken, A., Wemmer, K., 2003. Provenance and tectonic setting of the protoliths of the Metamorphic Complexes of Sierra de San Luis. Revísta de la Asociación Geológica Argentina 58 (4), 525–540.

López de Luchi, M.G., Rapalini, A.E., Siegesmund, S., Steenken, A., 2004. Application of magnetic fabrics to the emplacement and tectonic history of Devonian granitoids in Central Argentina. In: Martín- Hernández, F., Luneburg, C., Aubourg, C., Jackson, M. (Eds.), Magnetic Fabric: Methods and applications. Geological Society of London Special Publication, vol. 238, pp. 447–474.

López de Luchi, M., Siegesmund, S., Wemmer, K., Steenken, A., Naumann, R., 2007. Geochemical constraints on the petrogenesis of the Palaeozoic granitoids of the Sierra de San Luis, Sierras Pampeanas, Argentina. Journal of South American Earth Sciences 24 (2–4), 138–166.

Lork, A., Miller, H., Kramm, U., 1990. U–Pb zircon and monazite ages of the Angostura granite and the orogenic history of the northwest Argentine Basement. Journal of South American Earth Sciences 2, 147–153.

Lucassen, F., Becchio, R., Wilke, H.G., Franz, G., Thirlwall, M.F., Viramonte, J., Wemmer, K., 2000. Proterozoic–Paleozoic development of the basement of the Central Andes (18–26 S) – a mobile belt of the South American craton. Journal of South American Earth Sciences 13, 697–715.

Ludwig, K.R., 2000. SQUID 1.00, A User's Manual. Berkeley Geochronology Center Special Publications 2.

McLennan, S.M., 1989. Rare earth elements in sedimentary rocks: Influence of provenance and sedimentary process. Mineralogical Society of America, Reviews in Mineralogy 21, 169–200.

McLennan, S.M., 2001. Relationships between the trace element composition of sedimentary rocks and upper continental crust. Geochemistry, Geophysics, Geosystems 2. 2000GC000109.

McLennan, S.M., Taylor, S.R., McCulloch, M.T., Maynard, J.B., 1990. Geochemical and Nd–Sr isotopic composition of deep-sea turbidites: crustal evolution and plate tectonic associations. Geochimica et Cosmochimica Acta 54, 2015–2050.

McLennan, S.M., Hemming, S., McDaniel, D., Hanson, G., 1993. Geochemical approaches to sedimentation, provenance and tectonics. Geological Society of America Special Paper 284, 21–40.

Nance, W.B., Taylor, S.R., 1976. Rare earth element patterns and crustal evolution – I. Australian post-Archean rocks. Geochimica et Cosmochimica Acta 40, 1539–1551.

Nesbit, H.W., Young, G.M., 1982. Early proterozoic climates and plate motions inferred from major element chemistry of lutites. Nature 299, 715–717.

Nesbit, H.W., Markovics, G., Price, R.C., 1980. Prediction of some weathering trends of plutonic and volcanic rocks based on thermodynamic and kinetic considerations. Geochimica et Cosmochimica Acta 44, 1659–1666.

Nesbit, H.W., Young, G.M., McLennan, S.M., Keays, R.R., 1996. Effects of chemical weathering and sorting on the petrogenesis of siliclastic sediments with implications for provenance studies. Journal of Geology 104, 525–542.

Omarini, R.H., 1983. Caracterización litológia, diferenciación y genesis de la Formación Puncoviscana entre el Valle de Lerma y la Faja Eruptiva de la Puna. Ph.D. Thesis, Universidad Nacionál de Salta, Argentina

Omarini, R.H., Sureda, R.J., Götze, H.J., Seilacher, A., Pflüger, F., 1999. Puncoviscana folded belt in northwestern Argentina: testimony of late Proterozoic Rodinia fragmentation and pre-Gondwana collisional episodes. International Journal of Earth Sciences 88, 76–97.

Ortiz Suárez, A., Prozzi, C.R., Llambías, E.J., 1992. Geología de la parte sur de la Sierra de San Luis y granitoides asociados, Argentina. Estudios Geológicos 48, 269–277.

Pankhurst, R.J., Rapela, C.W., 1998. The Proto-Andean Margin of Gondwana: An Introduction. In: Pankhurst, R.J., Rapela, C.W. (Eds.), The Proto-Andean Margin of Gondwana. Geological Society of London Special Publications, Vol. 142, pp. 1–9.

Pankhurst, R.J., Ramos, A., Linares, E., 2003. Antiquity and evolution of the Río de la Plata craton in Tandilia, southern Buenos Aires province, Argentina. Journal of South American Earth Sciences 16, 5–13.

Pankhurst, R.J., Rapela, C.W., Saavedra, J., Baldo, E., Dahlquist, J., Pascua, I., Fanning, C.M., 1998. The Famatinian magmatic arc in the central Sierras Pampeanas: an Early to Mid-Ordovician continental arc on the Gondwana margin. In: Pankhurst, R.J., Rapela, C.W. (Eds.), The Proto-Andean Margin of Gondwana. Geological Society of London, Special Publications, Vol. 142, pp. 343–367.

Preciozzi, F., Peel, E., Muzio, R., Ledesma, J.J., Guerequiz, R., 2001. Dom Feliciano belt and Punta del Este Terrane: Geochronological features. In: Third South American Symposium on Isotope Geology, Pucón, Chile, pp. 217–220.

Prozzi, C., Zimmermann, U., 2005. Provenance of metasedmientary successions of the sierra de San Luis: first results. Congresso Geológico Argentino 16.

Prozzi, C.R., Ramos G., 1988. La Formación San Luis. In: First Jornadas de trabajo de Sierras Pampeanas, San Luis Abstracts, p. 1.

Ramos, V.A., 1988. Late Proterozoic–early Paleozoic of South America: a collisional story. Episodes 11, 168–174.

Ramos, V.A., 2008. The basement of the Central Andes: the Arequipa and related Terranes. Annual review of Earth and Planetary Sciences 36, 289–324.

Ramos, V.A., Jordan, T.E., Allmendinger, W., Mpodozis, C., Kay, S.M., Cortés, J.M., Palma, M., 1986. Paleozoic terranes of the Central Argentine–Chilean Andes. Tectonics 5, 855–880.

Ramos, V.A., Escayola, M., Mutti, D.I., Vujovich, G.I., 2000. Proterozoic–early Paleozoic ophiolites of the Andean basement of southern South America. Geological Society of America, Special Paper 349, 331–349.

Ramos, V.A., Cristallini, E.O., Pérez, D.J., 2002. The Pampean flat-slab of the Central Andes. Journal of South American Earth Sciences 15, 59–78.

Rapela, C.W., 2000. The Sierras Pampeanas of Argentina: Paleozoic building of the southern Proto-Andes. In: Cordani, U.G., Milani, E.J., Thomas-Filho, A., Campos, D.A. (Eds.), Tectonic Evolution of South America, 31st International Geological Congress, Río de Janeiro, pp. 381–387.

Rapela, C.W., Toselli, A.J., Heaman, L., Saavedra, J., 1990. Granite plutonism of the Sierras Pampeanas: an inner cordilleran Paleozoic arc in the southern Andes. Geological Society of America, Special Paper 241, 77–90.

Rapela, C.W., Pankhurst, R.J., Casquet, C., Baldo, E., Saavedra, J., Galindo, C., Fanning, C.M., 1998. The Pampean Orogeny of the southern proto-Andes: Cambrian continental collision in the Sierras de Córdoba. In: Pankhurst R.J., Rapela C.W. (Eds.), The Proto-Andean Margin of Gondwana Geolgical Society of London Special Publications, vol. 142, pp. 181–217.

Rapela, C.W., Pankhurst, R.J., Casquet, C., Fanning, C.M., Baldo, E.G., Gonzáles-Casado, J.M., Galindo, C., Dahlquist, J., 2007. The Río de la Plata craton and the assembly of Gondwana. Earth-Science Reviews 83, 49–82.

Roser, B.P., Korsch, R.J., 1988. Provenance signatures of sanstone-mudstone suites determined using discrimination functions analyses of major element data. Chemical Geology 67, 119–139.

Roser, B.P., Cooper, R.A., Nathan, S., Tulloch, A.J., 1996. Reconnaissance sandstone geochemistry, provenace and tectonic setting of the lower Paleozoic terranes of the West Coast and Nelson, New Zealand. New Zealand Journal of Geology and Geophysics 39, 1–16.

Rossi de Toselli, J.N., Durand, F.R., Toselli, A.J., Sardi, F.G., 1997. Aspectos estratigráficos y geocímicos comparatives del basamento metamórfico de bajo grado del Sistema de Famatina, Argentina. Revista de la Asociación Geológica Argentina 52, 469–480.

Rozendaal, A., Gresse, P.G., Scheepers, R., Le Roux, J.P., 1999. Neoproterozoic to Early Cambrian crustal evolution of the Pan-African Saldania belt, South Africa. Precambrian Research 97, 303–323.

Sato, A.M., González, P., Sato, K., 2001. First indication of Mesoproterozoic age from the western basement of the Sierra de San Luis, Argentina, 3rd South American Symposium on Isotope Geology, Extended Abstracts (CD edition), Sociedad Geológica de Chile, Santiago, pp. 64–67.

Sato, A.M., Gonzáles, P.D., Basei, M.A.S., Llambias, E.J., 2006. U–Pb ages of Komatiitic Rocks from Sierra de San Luis, Argentina. In; Fifth South American Symposium on Isotope Geology, Short Papers, pp. 169–173.

Scheepers, R., Armstrong, R., 2002. New U–Pb SHRIMP zircon ages of the Cape Granite Suite: implications for the magmatic evolution of the Saldania belt. South African Journal of Geology 105, 241–256.

Schwartz, J.J., Gromet, L.P., 2004. Provenance of a late Proterozoic–early Cambrian basin, Sierras de Córdoba, Argentina. Precambrian Research 129, 1–21.

Schwartz, J.J., Gromet, L.P., Miro, R., 2008. Timing and duration of the calc-alkaline arc of the Pampean orogeny: implications for the late Neoproterozoic to Cambrian Evolution of Western Gondwana. The Journal of Geology 116, 39–61.

Siegesmund, S., Steenken, A., Martino, R. Wemmer, K. López de Luchi, M.G., Frei R., Presniakov, S., Guereschi, A., 2009. Time constraints on the tectonic evolution of the Eastern Sierras Pampeanas (Central Argentina). International Journal of Earth Sciences, in press.

Sims, J.P., Sikkorow, R.G., Stuart-Smith, P.G., Lyons, P., 1997. Informe geológico y metalogenético de las Sierras de San Luis y Comechingones (provincias de San Luis y Córdoba), 1:250000. Anales 28, IGRM, SEGEMAR, Buenos Aires, pp. 1–148.

Sims, J.P., Ireland, T.R., Cmacho, A., Lyons, P., Pieters, P.E., Skirrow, R.G., Stuart-Smith, P.G., Miró, R., 1998. U–Pb, Th–Pb and Ar–Ar geochronology form the southern Sierras Pampeanas: implication for the Palaeozoic tectonic evolution of the western Gondwana margin. In: Pankhurst, R.J., Rapela, C.W. (Eds.), The Proto-Andean Margin of Gondwana. Geological Society of London Special Publication, vol. 142, pp. 259–281.

Söllner, F., de Brodtkorb, M.K., Miller, H., Pezzutti, N.E., Fernaández, R.R., 2000. U–Pb zircon ages of metavolcanic rocks from the Sierra de San Luis, Argentina. Revista de la Asociación Geológica Argentina 55 (1–2), 15–22.

Steenken, A., López de Luchi, M.G., Siegesmund, S., Wemmer, K., Pawlig, S., 2004. Crustal provenance and cooling of the basement complexes of the Sierra de San Luis: an insight into the tectonic history of the proto-Andean margin of Gondwana. Gondwana Research 7 (4), 1171–1195.

Steenken, A., López de Luchi, M.G., Martino, R.D., Siegesmund, S., Wemmer, K., 2005. SHRIMP dating of the El Peñón granite: a time marker at the turning point between the Pampean and Famatinian cycles within the Conlara Metamorphic Complex (Sierra de San Luis; Argentina)? In: 16th Congreso Geológico Argentino. Actas, vol. 1, pp. 889–896.

Steenken, A., Siegesmund, S., López de Luchi, M.G., Frei, R., Wemmer, K., 2006. Neoproterozoic to early Palaeozoic events in the Sierra de San Luis: implications for the Famatinian geodynamics in the Eastern Sierras Pampeanas (Argentina). Journal of the Geological Society 163, 965–982.

Steenken, A., López de Luchi, M.G., Siegesmund, S., Wemmer, K., Naumann, R., 2007. Geochemical constraints on the petrogenesis of the Paleozoic granitoids of the Sierra de San Luis, Sierras Pampeanas, Argentina. Journal of South American Earth Sciences 24, 138–166.

Steenken, A., Siegesmund, S., Wemmer, K., López de Luchi, M.G., 2008. Time constraints on the Famatinian and Achalian structural evolution of the basement of the Sierra de San Luis (Eastern Sierras Pampeanas, Argentina). Journal of South American Earth Sciences 25 (3), 336–358.

Stuart-Smith, P.G., Camacho, A., Sims, J.P., Skirrow, R.G., Lyons, P., Pieters, P.E., Black, L.P., 1999. Uranium–lead dating of felsic magmatic cycles in the southern Sierras Pampeanas, Argentina: implications for the tectonic development of the proto-Andean Gondwana margin. In: Ramos, V.A., Keppie, J.D. (Eds.), Laurentia–Gondwana Connections before Pangea. Geological Society of America, Special Papers, vol. 336, pp. 87–114.

Taylor, S.R., McLennan, S.M., 1981. The composition and evolution of the continental crust: rare earth element evidence from sedimentary rocks. Philosophical Transactions of the Royal Society A301, 381.

Taylor, S.R., McLennan, S.M., 1985. The Continental Crust: Its Composition and Evolution. Blackwell Science, Oxford.

Thomas, W., Astini, R., 2003. Ordovician accretion of the Argentine Precordillera terrane to Gondwana: a review. Journal of South American Earth Sciences 16, 67–79.

Thomas, W.A., Astini, R.A., Bayona, G., 2002. Ordovician collision of the Argentine Precordillera with Gondwana, independent of Laurentian Taconic Orogeny. Tectonophysics 345, 131–152.

Todt, W., Cliff, R.A., Hanser, A. & Hofmann, A.W. 1993. Re-calibration of NBS lead standards using a^{202} Pb + ^{205}Pb double spike. Terra Abstracts 5, Suppl. 1.

Toselli, A.J., 1990.Metamorfismo del Ciclo Pampeano. In: Aceñolaza, F.G., Miller, H., Toselli, A.J., (Eds.), El Ciclo Pampeano en el Noroeste Argentino. Universidad Nacionál de Tucumánn, Argentina, Serie Correlación Geológica, vol. 4, pp. 181–197.

Toselli, A.J., Aceñolaza, F.G., 1978. Geocronología de las Formaciones Puncoviscana y Suncho, Provincias de Salta y Catamarca. Revista de la Asociación Geológica Argentina 33, 76–80.

Tosdal, R.M., 1996. The Amazon–Laurentian connection as viewed from the Middle Proterozoic rocks in the central Andes, western Bolivia and northern Chile. Tectonics 15, 827–842.

Trindade, R.I.F., D'Agrella-Filho, M.S., Epof, I., Brito Neves, B.B., 2006. Paleomagnetism of early Cambrian Itabaiana mafic dikes (NE Brazil) and the final assembly of Gondwana. Earth and Planetary Science Letters 244, 361–377.

von Eynatten, H., Barceló-Vidal, C., Pawlowsky-Glahn, V., 2003. Composition and discrimination of sandstones: a stochastic evaluation of different analytical methods. Journal Sedimentary Research 73, 47–57.

von Gosen, W., Prozzi, C., 1998. Structural evolution of the Sierra de San Luis (Eastern Sierras Pampeanas, Argentina): implications for the Proto-Andean margin of Gondwana. In: Pankhurst, R.J., Rapela, C.W. (Eds), The Proto-Andean Margin of Gondwana Geological Society of London Special Publication, vol. 142, pp. 235–258.

Williams, I.S., 1998. U–Th–Pb geochronology by ion microprobe. In: McKibben, M.A., Shanks, W.C.P. III, Ridley, W.I. (Eds.), Applications of Microanalytical Techniques to Understanding Mineralizing Processes. Reviews in Economic Geology, vol. 7, pp. 1–35.

Willner, A.P., 1990. División tectonometamórfica del basamento del noroeste Argentino. In: Aceñolaza, F.G., Miller, H., Toselli, A.J. (Eds.), El Ciclo Pampeano en el Noroeste Argentino. Universidad Nacionál de Tucumánn, Argentina, Serie Correlación Geológica, vol. 4, pp. 113–159.

Willner, A.P., Miller, H., Ježek, P., 1985. Geochemical features of an Upper Precambrian–Lower Cambrian greywacke/pelite sequence (Puncoviscana trough) from the basement of the NW-Argentine Andes. Neues Jahrbuch für Geologie und Paläontologie Mitteilungen 33, 498–512.

Zimmermann, U., 1999. Sedimentpetrographische, geochemische und isotopengeochemische Methoden zur Bestimmung der Beziehung von Provenienz und Ablagerungungsraum an aktiven Kontinentalrändern: Das ordovizische back-arc Becken in der Süd-Puna, Hochland im Nordwesten Argentiniens. Ph.D. Thesis, University of Heidelberg, Germany

Zimmermann, U., Bahlburg, H., 2003. Provenance analyses and paleotectonic setting of the clastic Ordovician deposits in the southern Puna, NW Argentina. Sedimentology 50, 1079–1104.

Zimmermann, U., 2005. Provenance studies of very low to low-grade metasedimentary rocks of the Puncoviscana complex, northwest Argentina. In: Vaughan, A.P.M., Leat, P.T., Pankhurst, R.J. (Eds.), Terrane Processes at the Margin of Gondwana. Geological Society of London Special Publications, vol. 246, pp. 381–416.